

## ANNUAL REVIEWS Further

Click here to view this article's online features:

- Download figures as PPT slides
- Navigate linked references
- Download citations
- Explore related articles
- Search keywords

# Bacterial Hydrodynamics

Eric Lauga

Department of Applied Mathematics and Theoretical Physics, Center for Mathematical Sciences, University of Cambridge, Cambridge CB3 0WA, United Kingdom;  
email: e.lauga@damtp.cam.ac.uk

Annu. Rev. Fluid Mech. 2016. 48:105–30

The *Annual Review of Fluid Mechanics* is online at fluid.annualreviews.org

This article's doi:  
10.1146/annurev-fluid-122414-034606

Copyright © 2016 by Annual Reviews.  
All rights reserved

## Keywords

swimming bacteria, helical locomotion, low-Reynolds number flows,  
biological fluid dynamics

## Abstract

Bacteria predate plants and animals by billions of years. Today, they are the world's smallest cells, yet they represent the bulk of the world's biomass and the main reservoir of nutrients for higher organisms. Most bacteria can move on their own, and the majority of motile bacteria are able to swim in viscous fluids using slender helical appendages called flagella. Low-Reynolds number hydrodynamics is at the heart of the ability of flagella to generate propulsion at the micrometer scale. In fact, fluid dynamic forces impact many aspects of bacteriology, ranging from the ability of cells to reorient and search their surroundings to their interactions within mechanically and chemically complex environments. Using hydrodynamics as an organizing framework, I review the biomechanics of bacterial motility and look ahead to future challenges.

## 1. INTRODUCTION

**Flagellum:** organelle comprising the rotary motor, hook, and filament

Bacteria constitute the bulk of the biomass of our planet. However, because we need a microscope to see them, we often forget their presence. Observing life in the ocean, we see fish and crustaceans but miss the marine bacteria that outnumber them many times over. On land, we see animals and plants but often forget that a human body contains many more bacteria than mammalian cells. Although they are responsible for many infectious diseases, bacteria play a critical role in the life of soils and higher organisms (including humans) by performing chemical reactions and providing nutrients (Madigan et al. 2010).

Ever since microscopes were invented, scientists have worked to decipher the rules dictating the behavior of bacteria. In addition to quantifying the manner in which bacteria shape our lives and teach us about our evolutionary history, biologists have long recognized that the behavior of bacteria is influenced by the physical constraints of their habitat and by their evolution to maximize fitness under these constraints. The most prominent of these constraints is the presence of a surrounding fluid (Vogel 1996). Not only are all bacteria found in fluids, but being typically less than a hundredth of a millimeter in length, they experience much larger viscous forces than inertial forces and, as a result, have adapted their behavior.

Most bacteria are motile (Jarrell & McBride 2008, Kearns 2010), and this **motility is essential for the effectiveness of many pathogens** (Ottemann & Miller 1997). The most common form of bacterial motility is swimming. In order to swim, bacteria have evolved flagella (originally from secretory systems), consisting of slender helical appendages rotated by specialized motors and whose motions in viscous environments propel the cells forward (Bray 2000). The surrounding fluid can be seen both as a constraint and as an advantage. It is the presence of the fluid itself and its interactions with three-dimensional bacterial flagellar filaments that allows cells to move and sample their chemical environment—a crucial step for the cells to display robust and adaptive chemotactic responses to both attractants and repellents, for nutrients, but also to temperature, pH, and viscosity (Purcell 1977; Berg 1993, 2004; Blair 1995).

But as they self-propel, bacteria are subject to the external constraints set by the physical world and, in particular, by hydrodynamics. This review highlights the **consequences of fluid dynamics relevant to the swimming of bacteria in viscous environments**. Naturally, the biophysics of bacteria locomotion involves many aspects of soft matter physics, including nonlinear elasticity, screened electrostatics, interactions with diffusing chemicals, and biochemical noise; hence, fluid dynamics represents but one feature of the complex balance of forces dictating the behavior of cells as they search their environment. The choice made here is to use hydrodynamics as an organizing framework to overview various aspects of cellular locomotion.

Section 2 presents a biological overview of bacteria as cells, their geometry, the way they swim, and the variations among different species. Section 3 then reviews the basic hydrodynamic features of flagellar propulsion, which is followed by the flows induced by swimming bacteria in Section 4. Section 5 next addresses the polymorphs of flagellar filaments, their comparative hydrodynamics, and the potential relevance to the evolution of the flagellum. With individual flagella understood, Section 6 details how fluid forces may play a role in the actuation of multiple flagellar filaments and be used by cells to reorient. The last three sections are devoted to locomotion near surfaces (Section 7), in external flows (Section 8), and in complex fluids (Section 9).

Throughout this review, the **focus is on the mechanics of single-cell behavior**. Our purpose is to understand the way a single bacterium exploits, and is subject to, the physical constraints from the surrounding fluid. Other useful reviews can be used as complementary reading, in particular those highlighting the hydrodynamics of low-Reynolds number swimming (Lighthill 1975, Brennen & Winet 1977, Lauga & Powers 2009) and the fluid dynamics of plankton (Pedley & Kessler 1992,

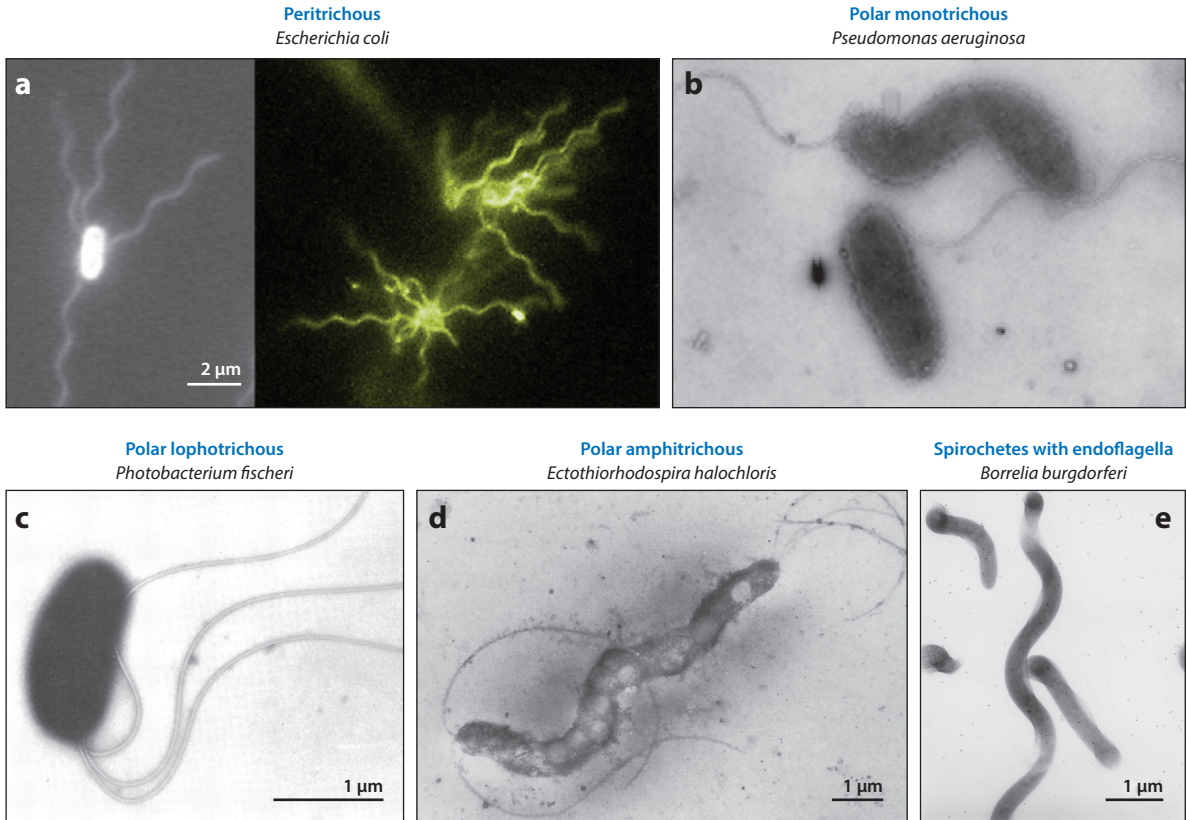


**Figure 1**

Atlas of flagellated bacteria. (a) Peritrichous *Escherichia coli*. Panel a, left, reproduced from Turner et al. (2000). Copyright 2000 American Society for Microbiology. Panel a, right, courtesy of H. Berg, Harvard University. (b) Polar monotrichous *Pseudomonas aeruginosa*. Panel b reproduced with permission from Fujii et al. (2008). Copyright 2008 Elsevier. (c) Polar lophotrichous *Photobacterium fischeri*. Panel c reproduced with permission from Allen & Baumann (1971). Copyright 1971 American Society for Microbiology. (d) Polar amphitrichous *Ectothiorhodospira halochloris*. Panel d reproduced with permission from Imhoff & Trüper (1977). Copyright 1977 Springer. (e) Spirochetes with endoflagella *Borrelia burgdorferi*. Panel e reproduced from with permission from Goldstein et al. (1996). Copyright 1996 American Society for Microbiology.

Guasto et al. 2012, Goldstein 2015), reproduction (Fauci & Dillon 2006, Gaffney et al. 2011), and collective cell locomotion (Koch & Subramanian 2011). Readers interested in the chemotactic aspects of bacteria locomotion are referred to the book by Berg (2004).

## 2. BIOLOGICAL ATLAS

Bacteria come in many different shapes (Madigan et al. 2010). Those able to swim in fluids can be roughly divided into two categories: bacteria whose propulsion is driven by helical flagellar filaments located outside a nondeforming cell body (the overwhelming majority; **Figure 1a-d**) and those with a spiral-like body undergoing time-varying deformation (**Figure 1e**).

Our understanding of how flagellated bacteria swim has its roots in a series of investigations in the 1970s showing conclusively that—unlike the flagella of eukaryotes, which are active and muscle-like (Bray 2000)—the **flagella of prokaryotes are passive organelles** (Berg & Anderson

**Flagellar filament:** helical polymeric filament whose rotational motion, driven by the rotary motor, enables bacterial locomotion

**Eukaryotes:** higher organisms whose cells have a nucleus; include all protists, plants, fungi, and animals

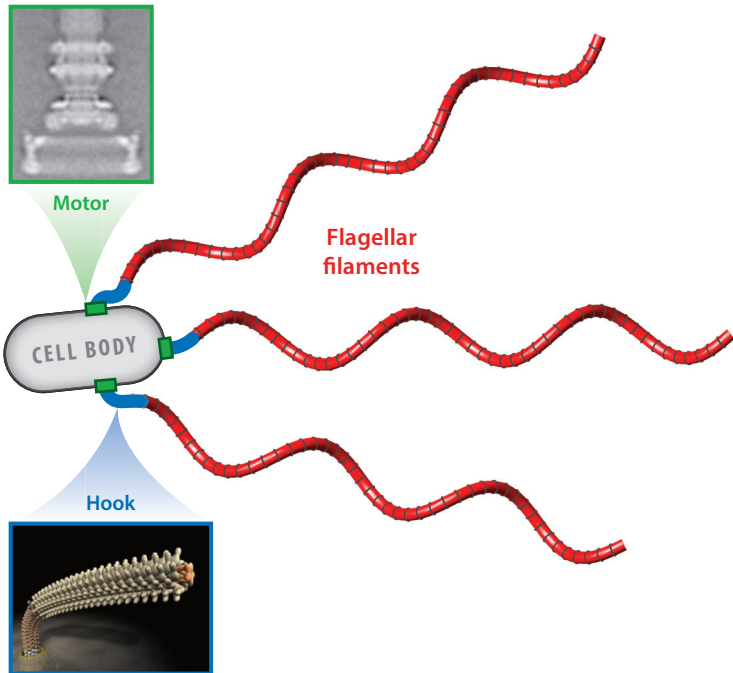


**Figure 2**

Schematic representation of a peritrichous bacterium with three flagellar filaments, showing a bacterial rotary motor embedded in the cell wall (the stator part of the motor is not shown) and a hook with its junction to a flagellar filament. Motor image reproduced with permission from Thomas et al. (2001). Copyright 2001 American Society for Microbiology. Hook image courtesy of K. Namba, Osaka University.

**Prokaryotes:** simple single-cell organisms that lack a nucleus; the majority of prokaryotes are bacteria

**Hook:** short flexible polymer acting as a universal joint between a rotary motor and a flagellar filament

**Rotary motor:** submicrometer stepper motor driven by ion fluxes embedded in the bacterial cell wall

**Peritrichous:** bacterium with many flagellar filaments driven by motors located at random locations on the cell walls

1973, Silverman & Simon 1974). Typically a few to ten micrometers in length, and only 40 nm in diameter, bacterial flagellar filaments are helical polymers whose structure is discussed in detail in Section 5. Each filament is attached to a short flexible hook ( $\approx$ 60 nm in length; see **Figure 2**) acting as a universal joint. The hook is turned by a stepper motor driven by ion fluxes (bacterial rotary motor; **Figure 2**), which is well characterized molecularly (Berg 2003).

Some flagellated cells are called peritrichous and have many motors (and thus many flagella) located randomly at various positions on the cell body (**Figure 1a**). This is the case for the bacterium *Escherichia coli*, chosen as a model organism to study the fundamental biophysical aspects of cell motility and chemotaxis (Berg 2004). In contrast, polar bacteria have motors located only at the poles of the body. Of the polar bacteria, monotrichous bacteria have only one motor, and thus one filament (**Figure 1b**); lophotrichous cells have a tuft of flagella originating from a single pole (**Figure 1c**); and amphitrichous bacteria have flagella at each pole (**Figure 1d**). Note that variations in this classification exist; for example, some monotrichous or lophotrichous bacteria are not polar. In all cases, the **rotation of the motor is transmitted to the hook, which in turn transmits it to the helical filament, leading to the generation of hydrodynamic propulsive forces**, as explained in detail in Section 3.

Fluid dynamics was used to determine the torque-frequency relationship for the rotary motor by linking tethered bacterial flagella to beads of different sizes in fluids of varying viscosity (Chen & Berg 2000). The resulting **change in the Stokes resistance to bead rotation** allowed the authors to show that the **rotary motor works at constant torque for a wide range of frequencies** in the

counterclockwise (CCW) direction (the frequency range strongly depends on temperature) before showing a linear decrease of the torque at higher frequencies (Berg 2003). In contrast, when rotating in the clockwise (CW) direction, the motor torque linearly decreases with the frequency (Yuan et al. 2010). In the range relevant to forward locomotion, the motor can be assumed to be continuously rotating and producing a constant CCW torque.

The value of this torque, however, is still under debate, and measurements are at odds with theoretical predictions. Whereas its stall torque has been experimentally estimated to be on the order of 4,600 pN nm (Berry & Berg 1997), experiments using beads lead to the conclusion that the motor has to be in the range  $1,260 \pm 190$  pN nm (Reid et al. 2006). In contrast, theoretical estimates using a simplified model for the fluid predict a significantly smaller value of  $370 \pm 100$  pN nm (Darnton et al. 2007).

Although the majority of swimming bacteria are powered by flagella rotating in the fluid outside the cells, two other modes of locomotion in fluids are notable. Bacteria of the spirochete family have a spiral shape and often undergo whole-body undulations also powered by flagella (Figure 1e). However, in this case, the flagella are constrained in the small space between the cytoplasmic membrane and the outer membrane of the cell body, and it is the rotation in this tight space that leads to wavelike, whole-body undulations. This in turn leads to locomotion in a fluid (Vig & Wolgemuth 2012). In contrast, some spirochetes are able to swim with no body deformation by inducing rotation of their outer membranes. Swimming without flagella has also been reported for *Spiroplasma*, a type of helical bacterium whose body has no cell wall. In that case, a wavelike motion is induced by contraction of the cell cytoskeleton, leading to the propagation of shape kinks along the body (Shaevitz et al. 2005, Wada & Netz 2007). At least one other bacterium, the marine *Synechococcus*, swims in fluids in a manner that is as yet undetermined (Ehlers & Oster 2012).

To close this biological overview, I mention the other mode of fluid-based motility, termed swarming (Jarrell & McBride 2008, Kearns 2010). When present in media that are rich in nutrients, a few bacterial families can undergo a differentiation to a swarming state, in which they become more elongated, grow more flagella, and swim in closely packed groups, the physics of which is only beginning to be unraveled (Copeland & Weibel 2009, Darnton et al. 2010).

### 3. HYDRODYNAMICS OF HELICAL PROPULSION

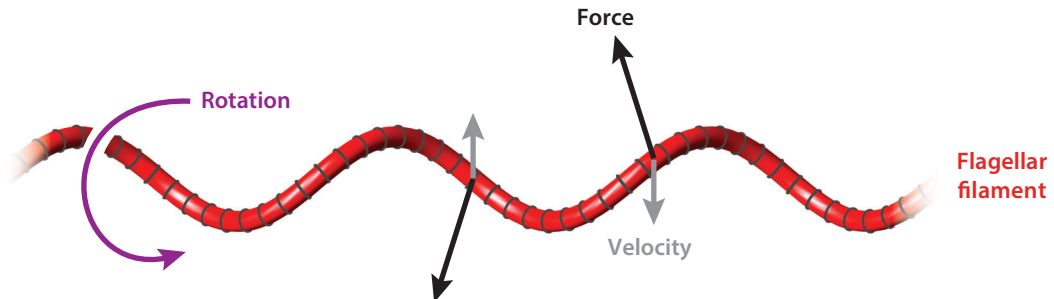
The most fundamental aspect of bacterial hydrodynamics is the ability of rotating flagella to produce propulsive forces (Chwang & Wu 1971, Lighthill 1976, Higdon 1979). At the origin of this force generation is the nonisotropic nature of hydrodynamic friction in the Stokesian regime (Brennen & Winet 1977, Lauga & Powers 2009). At the low Reynolds numbers relevant to swimming bacteria (typically ranging from  $10^{-4}$  to  $10^{-2}$ ), the flows are governed by the incompressible Stokes equations, and drag forces on rigid bodies scale linearly with their instantaneous velocities relative to the background fluid. Because flagellar filaments are slender (their aspect ratio is at least 100), their physics can be intuitively understood by analogy with the motion of a rod. At a given velocity, a rod experiences a drag from the fluid that is about twice as large when translating perpendicular to its long axis as that when moving along it. For a nonsymmetric velocity/rod orientation, the hydrodynamic drag on the rod is thus not aligned with the direction of its velocity but possesses a nonzero component perpendicular to it—hence the possibility of drag-based thrust.

Figure 3 illustrates the extension of this idea to the case of a helical filament. The flagellar filament is taken here to be left-handed and undergoes CCW rotation when viewed from the right looking left (discussed in Section 5). The local velocity of two material points on the helix is shown: Points in the foreground go down, whereas points in the background go up. The figure also shows the instantaneous drag force density resisting the rotation of the helix in the fluid. Because

**Polar:** bacterium with a small number of flagella attached at the poles of the cell body

**CCW:** counterclockwise

**CW:** clockwise



**Figure 3**

Hydrodynamics of propulsion by a rotating flagellum. A left-handed helix rotates in the counterclockwise direction (when viewed from the right), as indicated by the purple arrow. The local velocity of two material points on the helix relative to the background fluid is illustrated with gray arrows. Because the fluid drag is larger (for a given velocity) for motion of the local helix that is perpendicular than for motion parallel to the local tangent, the net force density from the fluid includes a component directed everywhere along the helix axis (black arrows). A net moment opposing the rotation is also generated, resulting in counter-rotation of the cell.

of the higher resistance from the projection of the local velocity in the direction perpendicular to the local tangent to the helix, the total drag includes a nonzero component along the axis of the helix, which in both cases points to the left along the helix axis (this is exaggerated in the figure for illustrative purposes). Consequently, a rotating helix is subject to a net viscous force aligned with the helix axis with an orientation that depends on the handedness of the helix and the direction of rotation.

From a Stokes flow standpoint, the grand resistance matrix for a helical filament, which linearly relates forces and moments to velocities and rotation rates, therefore includes an off-diagonal term coupling the axial rotation with axial force (Kim & Karrila 1991, Purcell 1997). Because the whole cell is force-free, it has to swim to balance this force. This is the physical mechanism used by bacteria to self-propel in fluids, and it will in fact be intuitive to anybody who has opened a bottle of wine with a corkscrew, for which the rotation of the screw induces its translation inside the cork. Differing from the case of the corkscrew, however, the propulsion of a helix in a viscous fluid produced by its rotation is very inefficient, both kinematically (small forward motion per rotation) and energetically (only a few percent of the total work done by the helix is transmitted to propulsive work) (Purcell 1997, Chattopadhyay et al. 2006, Spagnolie & Lauga 2011). The same hydrodynamic principles can be exploited to design artificial helical swimmers powered by rotating magnetic fields (Ghosh & Fischer 2009, Zhang et al. 2010). A famous illustration of helical locomotion in fluids is provided in G.I. Taylor's (1967) movie on low-Reynolds number flows.

In addition to forces, the rotating flagellum in **Figure 3** is subject to a net hydrodynamic moment resisting the rotation. For the bacterium to remain torque-free, the cell body therefore needs to counter-rotate. With flagella typically rotating at  $\approx 100$  Hz, this is achieved by a counter-rotation at a smaller frequency,  $\approx 10$  Hz, owing to the small rotational mobility of a large cell body (Chwang & Wu 1971, Magariyama et al. 1995). Because of this balance of moments, locomotion powered by helical filament is not possible in the absence of a cell body, a result qualitatively different from locomotion induced by planar waving deformation, for which a head is not required (Lighthill 1975, Lauga & Powers 2009). The resulting motion of a bacterium in a fluid thus consists of flagella rotating, the cell body counter-rotating, and the whole cell moving forward approximately in a straight line, or in helices of small amplitude when the axes of the flagellar filaments are not aligned with that of the cell body (Keller & Rubinow 1976, Hyon et al. 2012). Note that in general, the cell body does not induce additional propulsion, which all results from

the flagella, unless it is the right shape and has the right orientation relative to the helical flagellum (Chwang et al. 1972, Liu et al. 2014b). Helical swimming of *E. coli* is illustrated experimentally in **Supplemental Video 1** (follow the **Supplemental Material** link from the Annual Reviews home page at <http://www.annualreviews.org>).

▶ Supplemental Material

The hydrodynamic theories developed to calculate the force distribution on rotating helical flagellar filaments are of three flavors (Brennen & Winet 1977, Lauga & Powers 2009). The first one historically considered the theoretical limit of very (exponentially) slender filaments to compute forces as a perturbation expansion in the logarithm of the aspect ratio of the filament. At leading order, this so-called resistive-force theory predicts that the local force density at one point along the filament is proportional to its local velocity relative to the fluid, with a coefficient of proportionality that depends on the relative orientation of the velocity with respect to the local tangent (Gray & Hancock 1955, Cox 1970, Lighthill 1975). This is therefore the natural extension of the physical picture discussed above for rigid rods to deforming filaments. Although this is the most widely used approach, and one that is able to provide basic physical pictures, it is often not sufficiently accurate as the associated relative errors are only logarithmically small (Johnson & Brokaw 1979, Chattopadhyay & Wu 2009). More precise is the second approach, termed slender-body theory, which consists of distributing appropriate flow singularities of suitable strengths to match the boundary condition on the surface of the filament at a required, algebraically small, precision (Hancock 1953, Lighthill 1976, Johnson 1980). In that case, the equation relating the velocity distribution to the force distribution is nonlocal because of long-range hydrodynamic interactions, and thus needs to be inverted numerically. The third option is to use fully three-dimensional computations. The most common method is an integration of the equations of Stokes flows using boundary elements (Phan-Thien et al. 1987, Liu et al. 2013), regularized flow singularities (Flores et al. 2005, Olson et al. 2013), or immersed boundaries (Fauci & Dillon 2006). Mesoscopic particle-based methods have recently been proposed as an alternative approach (Reigh et al. 2012).

#### 4. FLOWS INDUCED BY BACTERIA

**Figure 4a** illustrates the general fluid dynamic picture of a swimming bacterium powered by the rotation of a flagellum. Near the flagellum, the induced flow is a combination of rotation and polar axial pumping directed away from the cell body. **Figure 4b,c** shows this using slender-body theory for a helical waveform of diameter 400 nm and wavelength 2.3  $\mu\text{m}$  (the so-called normal waveform; see discussion in Section 5) (Spagnolie & Lauga 2011).

Looking further away from the cell, because the swimming bacterium is force-free, it pushes on the fluid with an equal and opposite force to the one generated by the rotating flagellum (**Figure 4a**), and thus the leading-order flow in the far field is a force dipole, or stresslet (**Figure 4c**) (Batchelor 1970, Ishikawa et al. 2007). The type of associated dipole is termed a pusher, in contrast with puller dipoles relevant to cells that swim flagella first (e.g., planktonic biflagellates) (Guasto et al. 2012). This flow has been measured for swimming *E. coli* using an experimental tour de force (Drescher et al. 2011). The magnitude of the induced flow is shown in **Figure 4e** (in micrometers per second), and the theoretical dipolar prediction is shown in **Figure 4f**, with the difference between the two shown in **Figure 4g**. The dipole strength is on the order of 0.1–1 N  $\mu\text{m}$  (Berke et al. 2008, Drescher et al. 2011), and this dipolar picture is quite accurate up to a few body lengths away, at which point the flow speeds become overwhelmed by thermal noise.

Whereas the leading-order flow is a stresslet decaying spatially as  $1/r^2$ , the velocity field around a bacterium also includes higher-order (decaying as  $1/r^3$ ) flow singularities that are important in

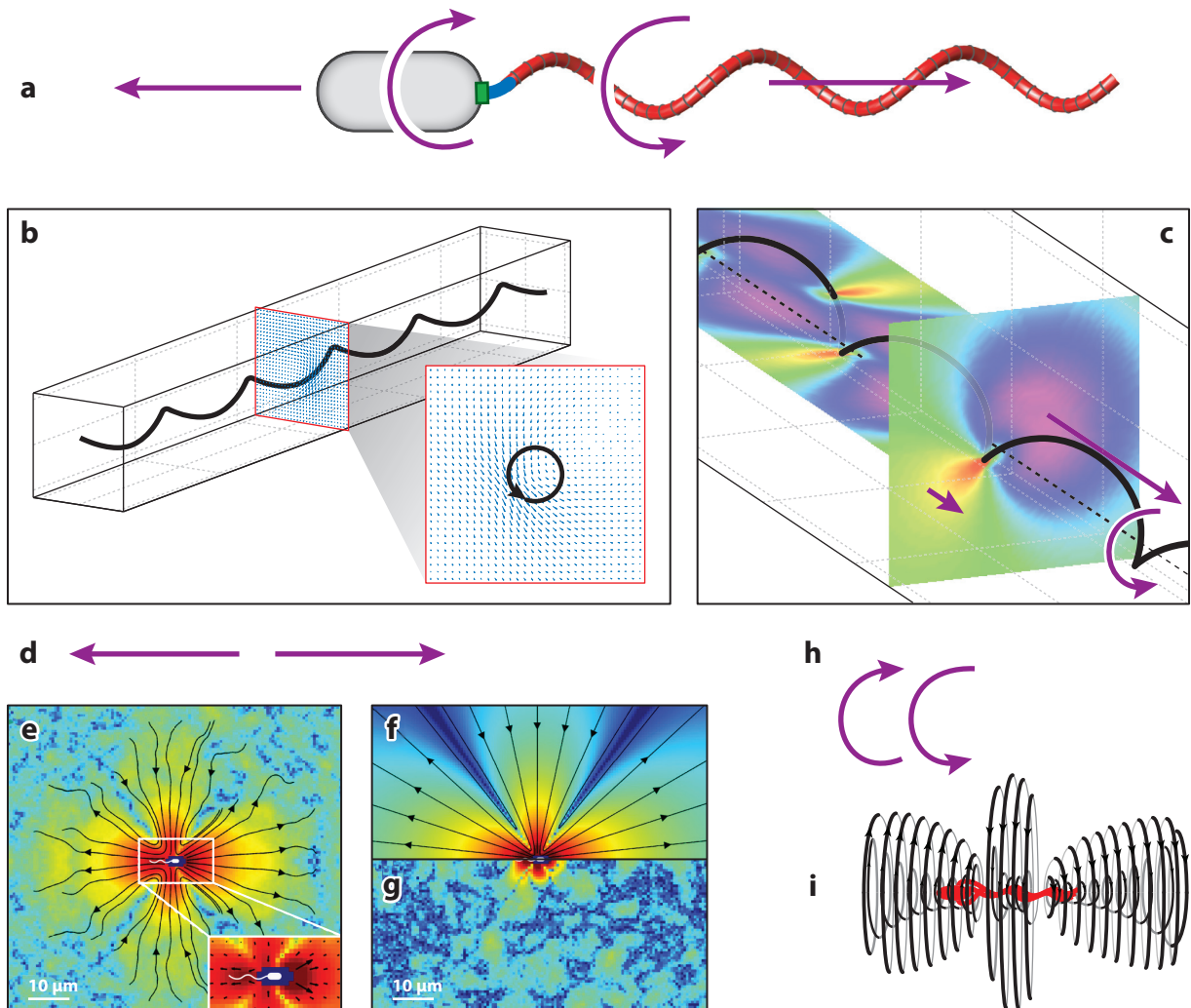


**Figure 4**

The flows produced by swimming bacteria. (a) Schematic representation of the forcing induced locally by the bacterium on the surrounding fluid (purple arrows). (b) Rotational flow near a rotating helical filament. (c) Axial flow along the axis of the helical filament, directed away from the cell body. Panels b and c reproduced with permission from Spagnolie & Lauga (2011). Copyright 2011 The American Physical Society. (d) In the far field, the cell acts on the fluid as a force dipole. (e) Measurement of the flow induced by swimming *Escherichia coli*. (f) Theoretical prediction from force dipole. (g) Difference between measurement and theoretical prediction. Panels e–g reproduced with permission from Drescher et al. (2011). (h) The rotation of the helical flagellum and the counter-rotation of the cell body acting on the fluid as a rotlet dipole. (i) Simulation of this rotational flow with streamlines. Panel i reproduced with permission from Watari & Larson (2010). Copyright 2010 Elsevier.

the near field. These include source dipoles and force quadrupoles (Chwang & Wu 1975). Force quadrupoles, for example, dominate velocity correlations between swimming bacteria because force dipoles are front-back symmetric (Liao et al. 2007). An important flow near a swimming bacterium is a rotlet dipole, which is a particular force quadrupole. Because the flagellum and the cell body rotate relative to the fluid in opposite directions (Figure 4a), they act on the fluid as two point moments (or rotlets) of equal and opposite strengths. Figure 4b schematically illustrates the

resulting rotlet dipole, decaying spatially as  $1/r^3$ . A computational illustration of the streamlines associated with this flow is shown in **Figure 4i** (Watari & Larson 2010). Both the force dipole and the rotlet dipole can be time dependent and in some cases induce instantaneous flows stronger than their time averages (Watari & Larson 2010).

The flows induced by swimming cells have been useful in understanding two problems. First, flows created by populations of bacteria lead to enhanced transport in the fluid. In addition to Brownian motion, passive tracers (e.g., nutrient molecules, or much larger suspended particles) also feel the sum of all hydrodynamic flows from the population of swimming bacteria and in general thus display an increase in the rate at which they are transported. Enhanced diffusion by swimming bacteria was first reported experimentally for flagellated *E. coli* cells with non-Brownian particles (Wu & Libchaber 2000), followed by work on molecular dyes (Kim & Breuer 2004). Dilute theories and simulations based on binary collisions between swimmers (possibly with a finite persistence time or finite run length) and passive tracers (possibly Brownian) have allowed the prediction of diffusion constants (Lin et al. 2011, Miño et al. 2013, Pushkin et al. 2013, Kasyap et al. 2014). In particular, it was shown that the extra diffusivity remains linear with the concentration of bacteria well beyond the dilute regime. The effect, although negligible for small molecules with high Brownian diffusivity, can be significant for large molecules or non-Brownian tracers.

The second problem for which swimming-induced flows are critical is that of collective swimming. Suspensions of swimming bacteria display modes of locomotion qualitatively different from individual cells, with long orientation and velocity correlation lengths, instabilities, and an intrinsic randomness—a process recently referred to as bacterial turbulence. Building on the standard theoretical description for Brownian suspensions (Doi & Edwards 1988), the modeling approach consists of describing the populations of swimming bacteria as continua using a probability density function in orientation and position. Conservation of probability then establishes a balance between changes in bacteria configurations and diffusion, with changes in both position and orientation that are brought about by the flows (and their gradients) induced by the swimming bacteria. Given that the current article is focused on single-cell behavior, we refer readers to a recent article in this journal on the topic (Koch & Subramanian 2011) and a book (Spagnolie 2015, and references therein) for a more detailed overview.

**Polymorphism:**  
the ability of bacterial flagellar filaments to take one of 12 stable helical shapes as a function of the chemical environment and their state of mechanical stress

## 5. POLYMORPHISM AND THE EVOLUTIONARY ROLE OF HYDRODYNAMICS

It is one of nature's wonders that bacterial flagellar filaments exist only in discrete helical shapes called flagellar polymorphs (Calladine 1978, Namba & Vonderviszt 1997, Hasegawa et al. 1998). Each flagellar filament is a polymer comprising a single protein (flagellin), which assembles in long protofilaments. Eleven of these protofilaments wrap around the circumference of the filament. Because the flagellin (and thus each protofilament) exists in two distinct conformation states, an integer number of different conformations is available for the filament, of which only 12 are molecularly and mechanically stable (Calladine 1978, Srigiriraju & Powers 2006). These are the helical polymorphic shapes illustrated in **Figure 5a**. Of these 12 shapes, 2 are straight, and 10 are true helices. Of these 10 helices, 9 have been observed experimentally, induced by chemical, mechanical, or temperature modifications (Leifson 1960; Hotani 1980, 1982). Of the 10 nonstraight shapes, 3 are left-handed—including the most common one, termed normal, whose polymorphic number is 2—and seven are right-handed—including the important semicoiled, which is number 4, and curly, which is number 5.

The force-extension curves of individual flagellar filaments, as elastic bodies, and the transitions between the different polymorphs have been precisely characterized experimentally using optical

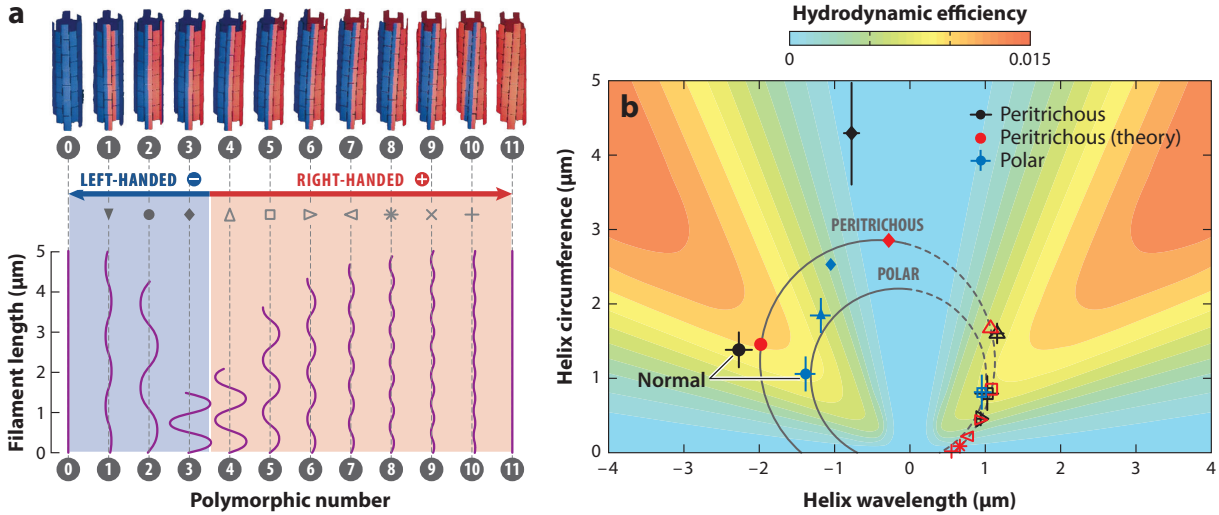


**Figure 5**

(a) Illustration of the 12 polymorphic shapes of bacterial flagellar filaments, numbered 0 to 11. Panel *a*, top, adapted with permission from Hasegawa et al. (1998). Copyright 1998 Elsevier. Panel *a*, bottom, adapted with permission from Darnton et al. (2007). Copyright 2007 Elsevier. (b) The intrinsic hydrodynamic efficiencies of each polymorph for Calladine's theory (red) and for experimentally measured peritrichous (black) and polar (blue) flagellar polymorphs. Left- (right) handed helices are denoted with negative (positive) wavelengths and the corresponding waveform with filled (empty) symbols, as given in panel *a*. The two large gray circles allow differentiating peritrichous from polar polymorphs. Panel *b* reproduced with permission from Spagnolie & Lauga (2011). Copyright 2011 American Physical Society.

tweezers pulling on filaments attached to a glass surface (Darnton & Berg 2007). Fitting the data to a Kirchhoff elastic rod model with multiple minima for curvature and twist allows then the determination of the elastic constants around polymorphic minima. The bending rigidities so estimated are on the order of few pN  $\mu\text{m}^2$ , and the transition forces from one shape to the next are on the order of a few pN (Darnton & Berg 2007). Various associated modeling approaches for flagellar mechanics have been developed to reproduce these experimental results (Wada & Netz 2008, Vogel & Stark 2010). That flagellar filaments are elastic means that they might deform under rotation, but during normal swimming conditions, this has been shown to be a small effect (Kim & Powers 2005). It is, however, possible that the moments and forces from the fluid induce the buckling of a rotating flagellar filament, similar to elastic rods buckling under their own weight. Although the threshold rotation rates appear to be close to biological numbers (Vogel & Stark 2012), no sign of filament buckling has been reported so far.

The fact that different shapes exist is important for locomotion because, as shown in the next section, when a bacterium turns, the direction of rotation of one (or more) bacterial motor is changing, which induces a rapid polymorphic transformation for the associated filament and, in particular, a flip of its chirality. This was modeled in a biophysical study for the bacterium *Rhodobacter sphaeroides* with two different polymorphs (Vogel & Stark 2013). Similar chirality transformations have been obtained in the lab using tethered flagella in external flows (Hotani 1982, Coombs et al. 2002). A helical flagellum held in a uniform stream is subject to a flow-induced tension as well as hydrodynamic moments, which are able to induce chirality reversal and cyclic transformations between right-handed (curly or semicoiled) and left-handed (normal) helices.

One aspect of polymorphism in which fluid dynamics plays a fascinating role is the propulsive performance of flagellar waveforms. For each waveform, an intrinsic propulsive efficiency may be

defined from the mobility matrix of the helix, comparing the power used for locomotion to the power expanded by the rotary motor against the fluid (Lighthill 1975, Purcell 1997). Physically, efficient helices are those that maximize the propulsive coupling between rotation and translation while minimizing the resistance in both translation and rotation. A near-rod helix, such as polymorph number 9 in **Figure 5a**, or one with a small wavelength, such as polymorph number 3, will be very inefficient. Which one of the different shapes is the most efficient? This is illustrated in **Figure 5b**, which plots the isovalues of the intrinsic hydrodynamic efficiency as a function of the helix wavelength and the circumference of the cylinder on which it is coiled (Spagnolie & Lauga 2011). Left-handed (right-handed) helices are denoted with negative (positive) wavelengths. Superimposed on the color map are the geometrical measurements from the actual polymorphs for both peritrichous and polar filaments together with the theoretical shapes predicted by molecular theories (Calladine 1978). The two large gray circles allow one to distinguish between peritrichous and polar polymorphs. In all cases, the most efficient waveform is the left-handed normal polymorph (number 2 in **Figure 5a**). This is the waveform displayed by bacteria during forward locomotion. Furthermore, not only is the normal helix the most efficient among all polymorphs, it is in fact close to being the overall optimal shape (which is at the intersection of the gray circles and the warm color in the map). In addition, further analysis of the results reveals that the second and third most efficient waveforms are the right-handed semicoiled (number 4 in **Figure 5a**) and curly (number 5) waveforms, both of which are used by wild-type swimming bacteria to change directions (see Section 6). These results suggest that fluid dynamics and mechanical efficiencies might have provided strong physical constraints in the evolution of bacterial flagella.

## 6. HYDRODYNAMICS OF REORIENTATIONS

Swimming is the mechanism that allows bacteria to sample their environment (Purcell 1977). Because they are small, bacteria are not able to sustain directional swimming for extended periods of time, and as a consequence, they always display diffusive behavior at long times. For swimming at speed  $U$  for a time  $\tau$  followed by a random change in direction, the long-time behavior is diffusive,  $r^2 \sim Dt$ , with the diffusivity scaling as  $D \sim U^2\tau$ , typically much larger than Brownian diffusivities (Berg 1993). When this diffusive dynamics is biased using sensing by the cells of their chemical environment, it leads to net drift and chemotaxis (Schnitzer 1993, Berg 2004).

The value of  $U$  is dictated by the hydrodynamics of swimming, but what sets the timescale  $\tau$ , and how do cells manage to reorient? The timescale is set internally by the sensing apparatus of bacteria, a complex but well-characterized internal protein network that chemically links the information gathered by receptors on the cell membrane to the action of the rotary motor (Falke et al. 1997). In order for the cells to then reorient, three mechanisms have been discovered, each taking advantage of different physics, and each involving fluid dynamics (Mitchell 2002).

The first mechanism is termed run and stop, in which a bacterium swims and then stops, simply waiting for thermal noise to reorient the cell. The timescale is therefore set in this case by a balance between the magnitude of thermal noise and the viscous mobility of the whole cell in rotation, leading to reorientation times on the order of seconds. The second mechanism, termed run and reverse, is used by many polar marine bacteria (Stocker & Seymour 2012). In that case, the rotary motor alternates between CCW and CW rotations. Kinematic reversibility for the surrounding fluid would predict that by doing so, the cells should keep retracing their steps. However, the propulsive forcing from the fluid on the flagellar filament, which is transmitted to the flexible hook, is able to induce buckling of the hook, which leads to a random reorientation of the cell, thereby escaping the reversibility argument (Xie et al. 2011, Son et al. 2013).

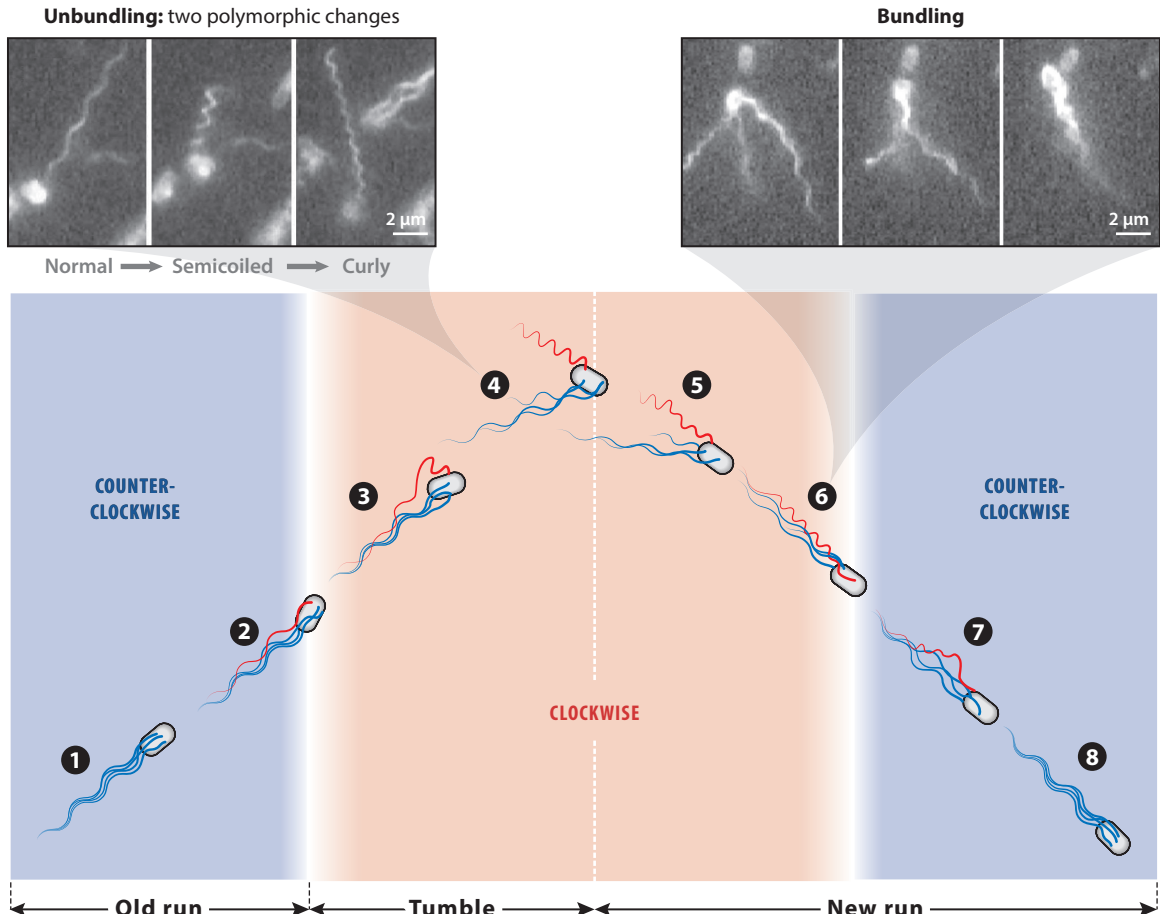


**Figure 6**

A run-to-tumble-to-run transition for swimming *Escherichia coli* as a model for the reorientation mechanism of peritrichous bacteria. During a run, all motors turn counterclockwise (blue). While in a tumble, at least one motor turns clockwise (red), which induces polymorphic changes in the associated flagellar filament, typically from normal to semicoiled and then curly (unbundling) before returning to the normal shape at the beginning of a new run (bundling). Figure adapted from Turner et al. (2000) and Darnton et al. (2007) with permission. Copyright 2000 and 2007 American Society for Microbiology.

The third, and most studied, mechanism is called run and tumble, used by peritrichous bacteria such as *E. coli*, whose details were made clear by a pioneering experiment allowing flagellar filaments to be visualized in real time (Turner et al. 2000) (see Figure 6). Critical to the effective locomotion in this case is the ability of multiple filaments to bundle when they all rotate in the same direction, and unbundle otherwise (Macnab 1977, Magariyama et al. 2001). When a bacterium runs, all its flagellar filaments adopt the normal waveform; turn in a CCW fashion (when viewed from behind the cell looking in); and are gathered in a tight, synchronized helical bundle behind the cell. Based on chemical clues from its environment, the cell might then initiate a tumbling event (which is Poisson distributed), for which at least one motor (but possibly more) switches its rotation direction to CW, inducing a polymorphic change in its filament from normal to semicoiled (in most cases), which at the same time flies out of the bundle, resulting in a change in orientation for the cell body. As the motor continues to rotate CW, the filament switches to the curly shape;

then when the motor reverts back to a CCW rotation, the filament comes back to the normal shape and returns into the bundle. These short tumbles typically last  $\tau \sim 0.1$  s, whereas the runs last approximately 1 s. **Supplemental Video 2** offers a visualization of run-and-tumble events for swimming *E. coli*. Note that many mutants of *E. coli* exist, either naturally occurring or genetically induced in the lab, displaying some variation in geometry or behavior; for example, the mutant HCB-437 does not tumble and is smooth swimming (Wolfe et al. 1988).

The bundling and unbundling of flagellar filaments constitute a large-deformation fluid-structure interaction problem at low Reynolds numbers combined with short-range filament-filament electrostatic repulsion (Weibull 1950, Lytle et al. 2002). Given this complexity, physical studies of bundling have taken two drastically different approaches. On the one hand, investigations have been carried out on very simplified geometries and setups, either numerically (Kim & Powers 2004, Reichert & Stark 2005) or experimentally at the macroscopic scale (Macnab 1977, Kim et al. 2003, Qian et al. 2009), to probe the synchronization between driven identical helices and their bundling. It was found that nonlocal hydrodynamic interactions between helices were sufficient to induce attraction, wrapping, and synchronization, provided the helices were of the right combination of chirality (both left-handed and rotating CCW or their mirror-image equivalent), but some amount of elastic compliance was required. Biologically, it was argued that this flexibility could be provided by the hook.

On the other hand, some groups have attempted to tackle the complexity of the problem using realistic setups of deforming flagella from various (often formidable) computational angles, including the use of regularized flow singularities (Flores et al. 2005), the immersed boundary method (Lim & Peskin 2012), mesoscale methods (Reigh et al. 2012), boundary elements (Kanehl & Ishikawa 2014), and bead-spring models adapted from polymer physics (Watari & Larson 2010, Janssen & Graham 2011). The numerical results confirm the physical picture of bundling and unbundling driven by a combination of flexibility and hydrodynamic interactions, with a critical dependence on the geometrical details, the relative configuration of the flagellar filaments, and the value of the motor torques driving the rotation.

## 7. BACTERIA SWIMMING NEAR SURFACES

Surfaces are known to affect the behavior of bacteria (Vanloosdrecht et al. 1990, Harshey 2003). One of the most striking aspects of locomotion near boundaries is the tendency of swimming bacteria to be attracted to surfaces, with steady-state concentration showing 10-fold increases near surfaces (Berke et al. 2008). **Figure 7a** illustrates this for smooth-swimming (i.e., nontumbling) *E. coli* cells. The attraction mechanism was first argued to be purely hydrodynamic in nature (Hernandez-Ortiz et al. 2005, Berke et al. 2008), easily understood as an image effect. As seen in Section 4, the flow perturbation induced by a swimming bacterium is (at leading order in the far field) a pusher force dipole. The hydrodynamic image system necessary to enforce a no-slip boundary condition on a flat surface includes a force dipole, a force quadrupole, and a source dipole, all located on the other side of the surface (**Figure 7b**) (Blake 1971). The net effect of these image singularities on the original dipole is a hydrodynamic attraction toward the wall. Intuitively, a pusher dipole draws fluid in from its side and therefore pulls itself toward a surface when swimming parallel to it. Similarly, the hydrodynamic moment induced by the image system is able to rotate pusher dipoles so that their stable orientation is swimming parallel to the surface (Berke et al. 2008), leading to kinematic asymmetries for bacteria switching between pusher and puller modes (Magariyama et al. 2005).

Experimental measurements of the flow induced by bacteria showed, however, that this dipolar flow is quickly overwhelmed by noise a few cell lengths away and thus acts only when the cells

## Supplemental Material

**Run and tumble:** the alternation between long swimming runs and short directional tumbles used by peritrichous bacteria to undergo random walks and search their environment

**Bundling:** process by which independently rotated flagellar filaments attract and synchronize to form a coherent bundle behind a swimming bacterium

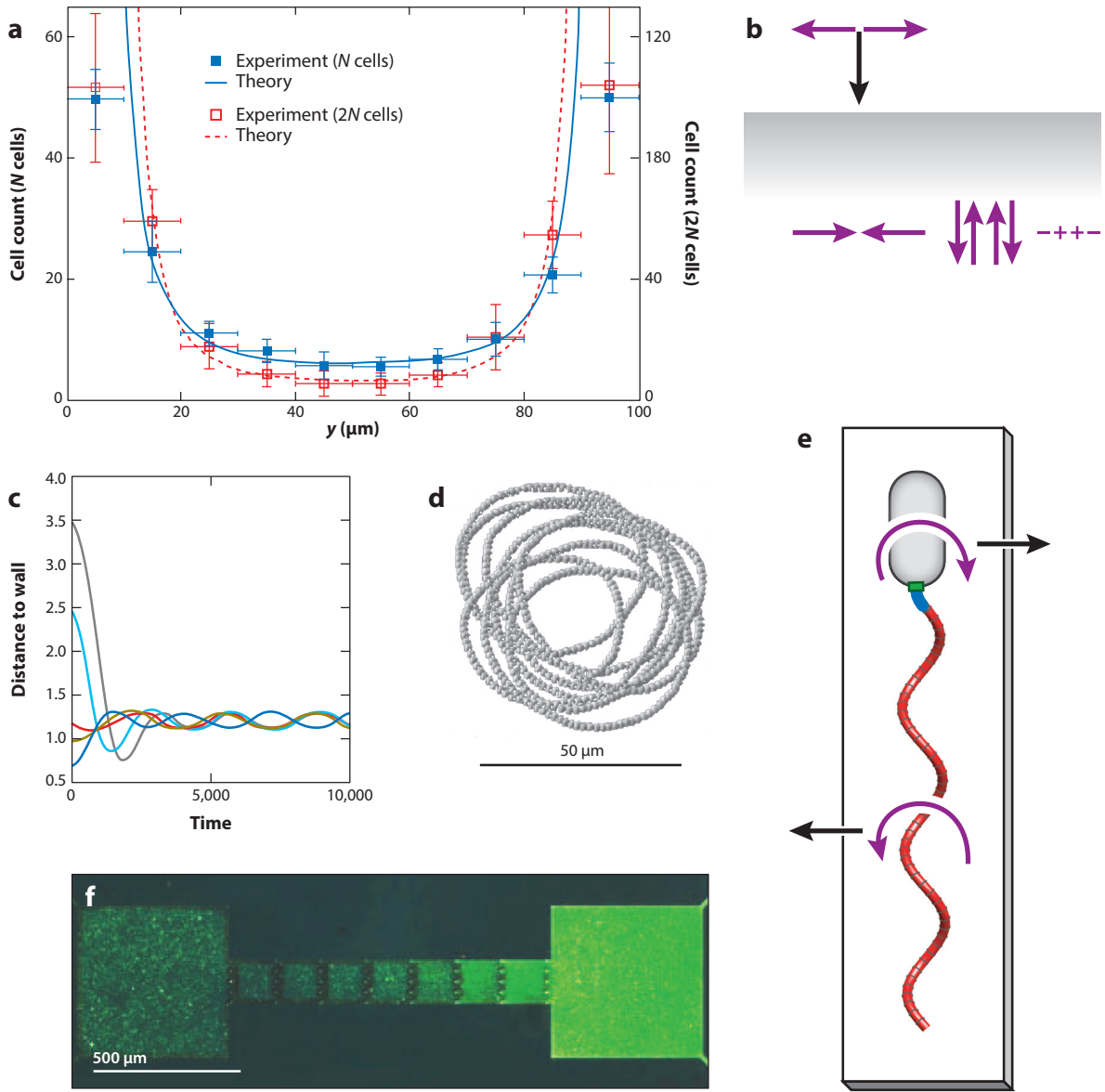


**Figure 7**

(a) Attraction of smooth-swimming *Escherichia coli* cells by two rigid surfaces located at  $y = 0$  and  $y = 100 \mu\text{m}$  (symbols) and fit by a point-dipole model (lines). Panel a adapted with permission from Berke et al. (2008). Copyright 2008 American Physical Society.

(b) Hydrodynamic images for a pusher force dipole above a flat no-slip surface (purple arrows) leading to attraction by the surface (black arrow).

(c) Computations showing stable swimming at a finite distance from a rigid surface for a model polar bacterium (distance to wall nondimensionalized by cell size as a function of time nondimensionalized by flagellar rotational frequency). Panel c adapted with permission from Giacché et al. (2010). Copyright 2010 American Physical Society.

(d) Tracking data for a smooth-swimming *E. coli* cell near a glass surface. Panel d adapted with permission from Vigeant & Ford (1997). Copyright 1997 American Society for Microbiology.

(e) Physical interpretation of a wall-induced moment on a bacterium with a helical flagellar filament leading to circular swimming. The rotating filament is subject to a surface-induced force to its left (when viewed from above) and the counter-rotating body by a force in the opposite direction, leading to a moment and therefore rotation of the cell.

(f) Rectification of fluorescent swimming *E. coli* in channels with asymmetric geometrical features. Panel f reproduced with permission from Galajda et al. (2007). Copyright 2007 American Society for Microbiology.

are close to the surface, leading to long residence times (Drescher et al. 2011). For cells that swim toward a surface and become trapped there, what determines the long-time equilibrium distance between the swimming cells and surfaces, and their orientation? Although simple models all predict that bacteria eventually touch walls, and therefore require short-range repulsion (Dunstan et al. 2012, Spagnolie & Lauga 2012), boundary element computations with a model polar bacterium demonstrated that hydrodynamics alone was able to select a stable orbit with swimming at a finite distance (**Figure 7c**) (Giacché et al. 2010).

A second remarkable feature of bacteria swimming near surfaces is a qualitative change in their trajectories. Between reorientation events, flagellated bacteria far from walls swim along straight or wiggly paths. Near rigid surfaces, their trajectories are observed to become circular, typically CW when viewed from above the surface in the fluid (Berg & Turner 1990, Frymier et al. 1995). **Figure 7d** illustrates this for an individually tracked *E. coli* cell swimming near a glass surface (Vigeant & Ford 1997). Early computations for model polar bacteria also predicted circular trajectories (Ramia et al. 1993), and recent experiments showed that the physicochemical nature of the interface plays a critical role in selecting the rotation direction (Lemelle et al. 2013, Morse et al. 2013).

The switch from forward to circular swimming is a fluid dynamic effect owing to new forces and moments induced near surfaces (Lauga et al. 2006). **Figure 7e** illustrates this for the locomotion of a model polar bacterium above a rigid wall. A helix rotating parallel to a no-slip surface is subject to a net force whose direction depends on the chirality of the helix and its direction of rotation (to the left in **Figure 7d** for a CCW rotation of a left-handed helix). Similarly, as the cell body is counter-rotating, it is subject to a hydrodynamic force in the direction of its rolling motion on the surface (to the right in **Figure 7d**) (Kim & Karrila 1991). These two forces are exactly zero far from the surface, and their magnitudes depend strongly on the distance to the wall (Li et al. 2008). The net effect of these forces is a wall-induced moment acting on the cell. Because the cell is torque-free, it needs to rotate (here, CW when viewed from above), leading to circular trajectories. Notably, the sign of the surface-induced forces is reversed if the rigid wall is replaced by a free surface, leading to circular swimming in the opposite direction (Di Leonardo et al. 2011), and a possible coexistence between CW and CCW motions for cell populations near complex interfaces (Lemelle et al. 2013, Morse et al. 2013, Lopez & Lauga 2014).

The interactions of bacteria with complex geometries have also led to fascinating results. Swimming *E. coli* cells in rectangular microchannels with three polymeric walls and one agar surface showed a strong preference to swim near the agar side of the channels (DiLuzio et al. 2005), a phenomenon still unexplained. The same bacteria are rectified by channels with asymmetric geometrical features (Galajda et al. 2007), which can then be exploited to passively increase cell concentrations (**Figure 7f**). Similarly, bacteria can be harnessed to perform mechanical work and, for example, rotate asymmetric microgears (Di Leonardo et al. 2010, Sokolov et al. 2010). In strong confinement, helical filaments continue to induce propulsion, but the swimming speed decreases for motion driven at constant torque (Liu et al. 2014a). Related experiments show that the limit of flagella-driven motility is reached when the cell body has a clearance of less than approximately 30% of its size, although cells can continue to move in smaller channels through cell division (Männik et al. 2009).

## 8. BACTERIA IN FLOWS

Similarly to colloidal particles, swimming bacteria respond to external flows by being passively advected and rotated. In many relevant situations in which the cells are much smaller than any of

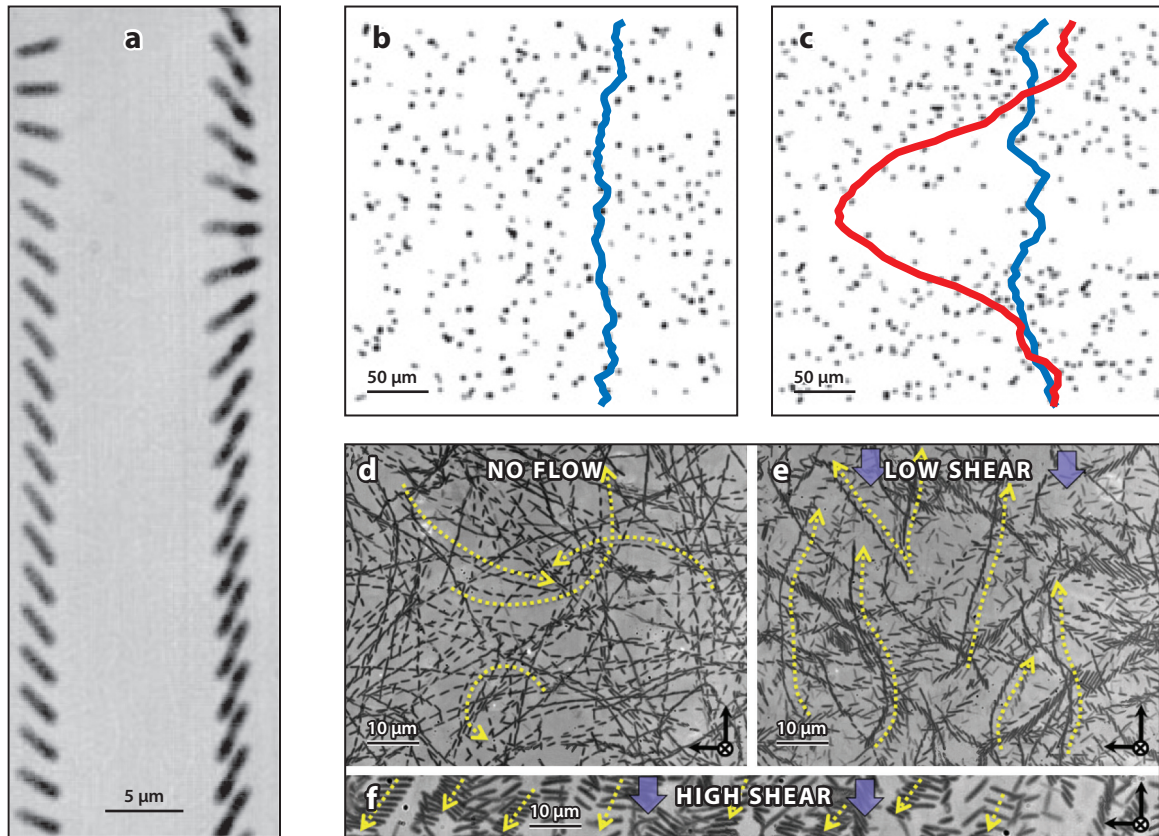


**Figure 8**

(a) Jeffery's orbits for nonflagellated *Escherichia coli* cells in a microchannel. Panel *a* reproduced with permission from Kaya & Koser (2009). Copyright 2009 American Physical Society. (b) Nonmotile *Bacillus subtilis* cells showing a uniform concentration under nonuniform shear. (c) Initially uniformly distributed motile cells (blue line). The cells then accumulate under nonuniform shear in the high-shear regions (red line). Panels *b* and *c* reproduced with permission from Rusconi et al. (2014). Copyright 2014 Macmillan Publishers Ltd. (d) Motile *E. coli* cells swimming in circles near rigid surfaces in the absence of flow. (e) Upstream swimming of the same cells under moderate shear. (f) The same cells under strong shear, in which all cells are advected downstream. Panels *d-f* reproduced with permission from Kaya & Koser (2012). Copyright 2012 Elsevier.

the flow length scales (e.g., in marine environments), the flow can be assumed to be locally linear and thus is a superposition of uniform translation, pure extension, and pure rotation. In that case, the dynamics of the (elongated) bacteria is described by Jeffery's equation, which is exact for prolate spheroids in linear flows (Pedley & Kessler 1992). Physically, the cells move with the mean flow velocity, and their rotation rate is the sum of the vorticity component (which alone would predict rotation at a constant rate) and the (potential) extensional component (which alone would predict steady alignment with the principal axes of extension). **Figure 8a** illustrates the resulting tumbling trajectories, called Jeffery's orbits, for nonflagellated *E. coli* cells under shear in a microfluidic device (Kaya & Koser 2009).

In addition to the classical Jeffery's orbits, bacteria are subject to another mechanism that results from their chiral shapes. The hydrodynamics of a helical flagellar filament in a simple shear flow

leads to a viscous torque being produced on the helix, which reorients it away from the plane of shear. Combined with motility, this is an example of rheotaxis, in which cells respond to shear (here, purely physically) (Marcos et al. 2012). Beyond the assumption of linear flow, swimming bacteria respond to nonuniform shears by developing nonuniform orientation distributions, which, when coupled to motility, lead to cells accumulating in the high-shear regions (Rusconi et al. 2014). **Figure 8b,c** illustrates this for *Bacillus subtilis* in a Poiseuille flow. Nonswimming cells have a uniform distribution (**Figure 8b**), whereas motile cells that start uniformly distributed develop nonuniform distributions and gather in the high-shear regions (**Figure 8c**).

One compelling aspect of the response of bacteria to external flows is the feedback of swimming cells on the surrounding fluid through the stresses they exert. Owing to their dipolar character, swimming bacteria exert bulk stresses on the fluid—hence the term stresslet originally coined by Batchelor (1970) in the context of passive suspensions. A group of swimming bacteria subject to an external deformation will thus generically respond by developing a state of stress with rich dynamics. The most fundamental question relating stresses to deformation in the fluid is, What is the effective viscosity of a suspension of swimming bacteria? Experiments were carried out with the peritrichous *B. subtilis* by estimating the viscosity in two different ways, first by looking at the unsteady decay of a vortex and then by directly measuring the torque on a rotating probe in the cell suspension (Sokolov & Aranson 2009). The results showed a strong reduction in the effective viscosity (up to a factor of seven), whereas an increase was possible at larger cell concentrations. A different setup was proposed for *E. coli* in which a suspension was caused to flow in a microchannel and the effective viscosity was estimated using predictions for the unidirectional velocity profile from multiphase Newtonian fluid dynamics (Gachelin et al. 2013). In that case, the effective viscosity showed an initial decrease, followed by shear thickening up to relative viscosities above 1, followed by shear thinning at high shear rates. In parallel, theoretical and computational work on model cells in both shear and extensional flows predicted a viscosity decrease for pusher cells, together with the possibility of negative viscosities and normal stress coefficients with a sign opposite to the ones for passive suspensions (Haines et al. 2009; Saintillan 2010a,b).

Finally, bacteria swimming near boundaries in external flows also have a propensity to swim upstream and hence against the flow (Cisneros et al. 2007, Hill et al. 2007). **Figure 8d–f** illustrates this for motile *E. coli* cells that swim in circles in the absence of flow (**Figure 8d**), move upstream under moderate shear (**Figure 8e**), and are passively advected downstream at high shear (**Figure 8f**) (Kaya & Koser 2012). The physical origin of this transition to upstream swimming has been proposed to be hydrodynamic, by which a shear flow of moderate strength produces a torque on a downward-facing cell that reorients it so that its stable equilibrium is to point upstream and thus swim against the flow (Hill et al. 2007, Kaya & Koser 2012).

## 9. LOCOMOTION IN COMPLEX FLUIDS

Bacteria that inhabit soils and higher organisms routinely have to progress through complex environments with microstructures whose characteristic length scales might be similar to that of the cell. Some bacteria also have to endure chemically and mechanically heterogeneous environments. For example, *Helicobacter pylori*, which survives in the acidic environment of the stomach, creates an enzyme that locally increases pH and can induce rheological changes to the mucus protecting the epithelium surface of the stomach, changing it from a gel to a viscous fluid in which it is able to swim (Bansil et al. 2013). In many instances, the surrounding fluids might not be totally flowing but might instead possess their own relaxation dynamics, which might occur on timescales comparable to the

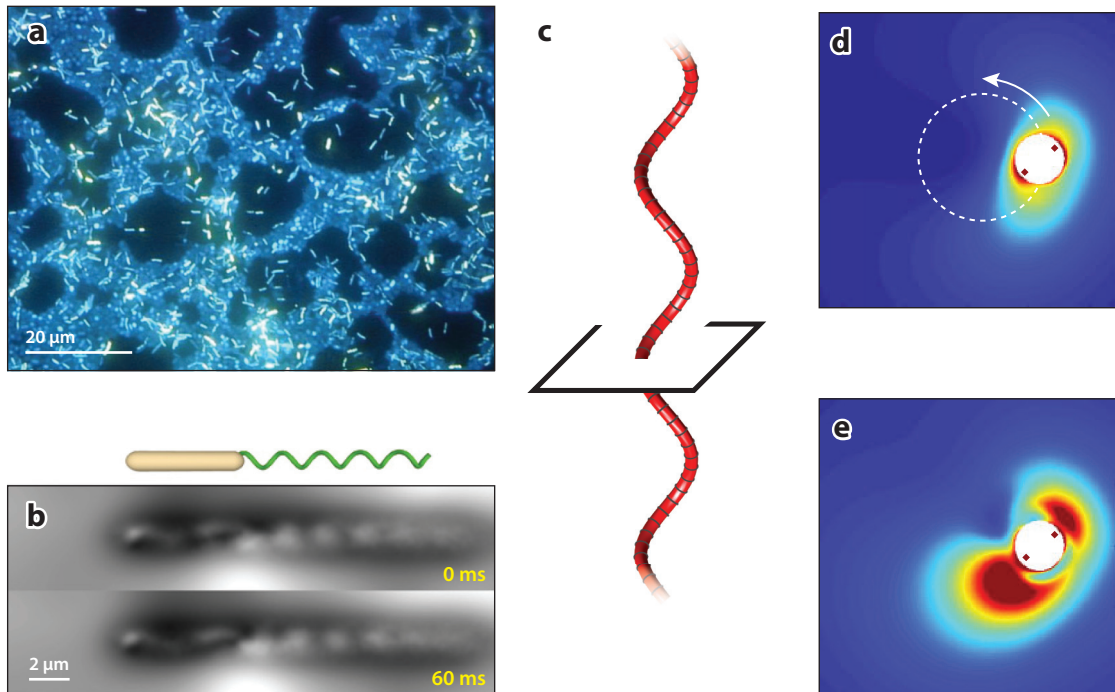


**Figure 9**

(a) Biofilm on the stainless steel surface of a bioreactor. Panel *a* courtesy of Centers for Disease Control and Prevention. (b) Waves in the director field created by rotating flagella of the peritrichous *Bacillus subtilis* in a liquid crystal. Panel *b* adapted with permission from Zhou et al. (2014). (c–e) Magnitude of the polymer stresses in the cross section of a model flagellar filament rotating in an Oldroyd-B fluid (nondimensionalized by the viscosity times the filament rotation rate) as obtained from computations. The white dashed line indicates the path followed by the filament centerline. The Deborah numbers are  $\text{De} = 0.3$  (*d*) and  $\text{De} = 1.5$  (*e*). Panels *d* and *e* adapted with permission from Spagnolie et al. (2013). Copyright 2013 American Physical Society.

intrinsic timescales of the locomotion. For example, during biofilm formation, bacteria produce an extracellular polymeric matrix for which they control the mechanical properties through water content (Costerton et al. 1995, Wilking et al. 2011) (Figure 9a). Several studies have attempted to quantify the impact of such complex fluids on the swimming kinematics and energetics of bacteria.

Early studies were concerned with perhaps the simplest question possible: How is bacterial locomotion modified by a change in the viscosity of the surrounding (Newtonian) fluid? Flagellated bacteria display a systematic two-phase response, in which an increase in viscosity is seen to first lead to a small increase in the swimming speed followed by a sharp decrease at large viscosities (Shoesmith 1960, Schneider & Doetsch 1974, Greenberg & Canale-Parola 1977). The decrease has been rationalized by assuming that the rotary motor is working at constant power output (Keller 1974), an assumption we now know is erroneous because it is the motor torque that is constant (see Section 2). In stark contrast with flagellated bacteria, spirochetes show a systematic enhancement of their swimming speed with an increase of the viscosity of the fluid (Kaiser & Doetsch 1975). In a related study, the viscosity required to immobilize bacteria was measured to be larger, by orders of magnitude, for spirochetes compared to that for flagellated bacteria (Greenberg & Canale-Parola 1977).

How can the difference between flagellated bacteria and spirochetes be rationalized? One argument brought forward focused on the details of the microstructure of the fluid, arguing that

all increases in viscosity are not created equal (Berg & Turner 1979). Increases in viscosity are induced by dissolving polymers, but the nature of the polymer chains' structure may be critical. Experiments showing large increases in swimming speeds used solutions of long unbranched chain polymers (e.g., methylcellulose), which are expected to form a network against which the cells are effectively able to push. In contrast, solutions of branched polymers are more homogeneous and should lead to a decrease of the swimming speed because, for a constant-torque motor rotating in a viscous fluid, the product of the viscosity and the rotational frequency needs to remain constant. The idea that the presence of the microstructure itself in the solvent is critical in explaining the change in swimming speeds was further modeled mathematically, with a similar physical picture (Magariyama & Kudo 2002, Leshansky 2009). Recent experiments shed further light on the interplay between the viscosity of the fluid and the torque applied by the rotary motor (Martinez et al. 2014). If the fluid is anisotropic (e.g., a liquid crystal), a strong coupling can develop between the director field and the bacteria, enabling constrained locomotion and fascinating novel flow features with truly long-ranged interactions (**Figure 9b**) (Zhou et al. 2014).

Recent work has focused on viscoelastic fluids with the primary motivation to understand the locomotion of bacteria, and higher organisms, in mucus (Lauga 2014). Such fluids have the added complexity of finite relaxation times,  $\lambda$ , and for flagella rotating with frequency  $\omega$ , a dimensionless Deborah number,  $De = \lambda\omega$ , needs to be considered. Small-amplitude theory on flagellar propulsion predicted that the relaxation in the fluid would always lead to slower swimming (Fu et al. 2007, Lauga 2007). Experiments with macroscopic helices driven in rotation and undergoing force-free translation confirmed the small-amplitude theoretical results but showed that helices with larger amplitudes could experience a moderate increase in the translational speed for Deborah numbers of order one (Liu et al. 2011). Detailed numerics on the same setup argued that the increase resulted from the rotating flagellar filament revisiting its viscoelastic wake, as illustrated in **Figure 9c–e** for  $De = 0.3$  and  $De = 1.5$  (Spagnolie et al. 2013).

## SUMMARY POINTS

1. Low-Reynolds number hydrodynamics is at the heart of the fundamental physics of bacteria swimming, first and foremost by the generation of propulsive forces. It might have also played a role in the evolution of the bacterial flagellum, resulting in optimal polymorphic shapes used for forward motion.
2. At the level of a single cell, fluid dynamic forces are exploited by peritrichous bacteria to induce fast bundling and unbundling of their multiple flagellar filaments, resulting in efficient reorientation mechanisms.
3. The flows created by swimming bacteria affect the interactions with their environment and with other cells, leading to enhanced nutrient transport and collective locomotion. Similarly, complex microstructures or external flows can have significant influence on the trajectories, concentrations, and orientations of swimming bacteria.
4. Although surrounding fluids play important roles in the life of bacteria, hydrodynamic forces on flagellar filaments and cell bodies often have to be balanced with bending and twisting elasticity, and short-range electrostatic interactions, and are subject to both biochemical and thermal noise. Fluid dynamics is therefore only one of the complex physical processes at play.

## FUTURE ISSUES

1. Why is the value of the experimentally measured torque applied by the rotary motor so different from that from hydrodynamic predictions (Darnton et al. 2007)? What are the other mechanical forces at play?
2. Why does the flagellar hook of peritrichous bacteria not buckle, as it does for polar bacteria under seemingly similar propulsive conditions (Son et al. 2013)? Why is the flagellar hook so precisely tuned in size and rigidity that flagellar bundling is no longer possible if small changes are made to it (Brown et al. 2012)?
3. How exactly can a tight bundle of multiple helical filaments open up and close repeatedly without jamming under the uncoordinated action of a few motors (Macnab 1977)? How much of this process is truly driven by hydrodynamic interactions versus other passive mechanisms?
4. Can we derive predictive whole-cell models that can reproduce the full run-and-tumble statistics of swimming bacteria based solely on our understanding of the behavior of rotary motors (Turner et al. 2000)?

## DISCLOSURE STATEMENT

The author is not aware of any biases that might be perceived as affecting the objectivity of this review.

## ACKNOWLEDGMENTS

I thank Tom Montenegro-Johnson for his help with the figures. Discussions with, and feedback from, Howard Berg, Ray Goldstein, and Tim Pedley are gratefully acknowledged. This work was funded in part by the European Union (through a Marie-Curie CIG Grant) and by the Isaac Newton Trust (Cambridge).

## LITERATURE CITED

- Allen RD, Baumann P. 1971. Structure and arrangement of flagella in species of the genus *Beneckeia* and *Photobacterium fischeri*. *J. Bacteriol.* 107:295–302
- Bansil R, Celli JP, Hardcastle JM, Turner BS. 2013. The influence of mucus microstructure and rheology in *Helicobacter pylori* infection. *Front. Immunol.* 4:310
- Batchelor GK. 1970. The stress system in a suspension of force-free particles. *J. Fluid Mech.* 41:545–70
- Berg HC. 1993. *Random Walks in Biology*. Princeton, NJ: Princeton Univ. Press
- Berg HC. 2003. The rotary motor of bacterial flagella. *Annu. Rev. Biochem.* 72:19–54
- Berg HC. 2004. *E. coli in Motion*. New York: Springer-Verlag
- Berg HC, Anderson RA. 1973. Bacteria swim by rotating their flagellar filaments. *Nature* 245:380–82
- Berg HC, Turner L. 1979. Movement of microorganisms in viscous environments. *Nature* 278:349–51
- Berg HC, Turner L. 1990. Chemotaxis of bacteria in glass capillary arrays: *Escherichia coli*, motility, microchannel plate, and light scattering. *Biophys. J.* 58:919–30
- Berke AP, Turner L, Berg HC, Lauga E. 2008. Hydrodynamic attraction of swimming microorganisms by surfaces. *Phys. Rev. Lett.* 101:038102
- Berry RM, Berg HC. 1997. Absence of a barrier to backwards rotation of the bacterial flagellar motor demonstrated with optical tweezers. *PNAS* 94:14433–37

- Blair DF. 1995. How bacteria sense and swim. *Annu. Rev. Microbiol.* 49:489–520
- Blake JR. 1971. A note on the image system for a stokeslet in a no-slip boundary. *Proc. Camb. Philos. Soc.* 70:303–10
- Bray D. 2000. *Cell Movements*. New York: Garland
- Brennen C, Winet H. 1977. Fluid mechanics of propulsion by cilia and flagella. *Annu. Rev. Fluid Mech.* 9:339–98
- Brown MT, Steel BC, Silvestrin C, Wilkinson DA, Delalez NJ, et al. 2012. Flagellar hook flexibility is essential for bundle formation in swimming *Escherichia coli* cells. *J. Bacteriol.* 194:3495–501
- Calladine CR. 1978. Change of waveform in bacterial flagella: the role of mechanics at the molecular level. *J. Mol. Biol.* 118:457–79
- Chattopadhyay S, Moldovan R, Yeung C, Wu XL. 2006. Swimming efficiency of bacterium *Escherichia coli*. *PNAS* 103:13712–17
- Chattopadhyay S, Wu X. 2009. The effect of long-range hydrodynamic interaction on the swimming of a single bacterium. *Biophys. J.* 96:2023–28
- Chen X, Berg HC. 2000. Torque-speed relationship of the flagellar rotary motor of *Escherichia coli*. *Biophys. J.* 78:1036–41
- Chwang AT, Wu TY. 1971. Helical movement of microorganisms. *Proc. R. Soc. B* 178:327–46
- Chwang AT, Wu TY. 1975. Hydromechanics of low-Reynolds-number flow. Part 2. Singularity method for Stokes flows. *J. Fluid Mech.* 67:787–815
- Chwang AT, Wu TY, Winet H. 1972. Locomotion of *Spirilla*. *Biophys. J.* 12:1549–61
- Cisneros LH, Cortez R, Dombrowski C, Goldstein RE, Kessler JO. 2007. Fluid dynamics of self-propelled microorganisms, from individuals to concentrated populations. *Exp. Fluids* 43:737–53
- Coombs D, Huber G, Kessler JO, Goldstein RE. 2002. Periodic chirality transformations propagating on bacterial flagella. *Phys. Rev. Lett.* 89:118102
- Copeland MF, Weibel DB. 2009. Bacterial swarming: a model system for studying dynamic self-assembly. *Soft Matter* 5:1174–87
- Costerton JW, Lewandowski Z, Caldwell DE, Korber DR, Lappinscott HM. 1995. Microbial biofilms. *Annu. Rev. Microbiol.* 49:711–45
- Cox RG. 1970. The motion of long slender bodies in a viscous fluid. Part 1. General theory. *J. Fluid Mech.* 44:791–810
- Darnton NC, Berg HC. 2007. Force-extension measurements on bacterial flagella: triggering polymorphic transformations. *Biophys. J.* 92:2230–36
- Darnton NC, Turner L, Rojevsky S, Berg HC. 2007. On torque and tumbling in swimming *Escherichia coli*. *J. Bacteriol.* 189:1756–64
- Darnton NC, Turner L, Rojevsky S, Berg HC. 2010. Dynamics of bacterial swarming. *Biophys. J.* 98:2082–90
- Di Leonardo R, Angelani L, Dell'Arciprete D, Ruocco G, Iebba V, et al. 2010. Bacterial ratchet motors. *PNAS* 107:9541–45
- Di Leonardo R, Dell'Arciprete D, Angelani L, Iebba V. 2011. Swimming with an image. *Phys. Rev. Lett.* 106:038101
- DiLuzio WR, Turner L, Mayer M, Garstecki P, Weibel DB, et al. 2005. *Escherichia coli* swim on the right-hand side. *Nature* 435:1271–74
- Doi M, Edwards SF. 1988. *The Theory of Polymer Dynamics*. New York: Oxford Univ. Press
- Drescher K, Dunkel J, Cisneros LH, Ganguly S, Goldstein RE. 2011. Fluid dynamics and noise in bacterial cell-cell and cell-surface scattering. *PNAS* 108:10940–45
- Dunstan J, Miño G, Clément E, Soto R. 2012. A two-sphere model for bacteria swimming near solid surfaces. *Phys. Fluids* 24:011901
- Ehlers K, Oster G. 2012. On the mysterious propulsion of *Synechococcus*. *PLOS ONE* 7:e36081
- Falke JJ, Bass RB, Butler SL, Chervitz SA, Danielson MA. 1997. The two-component signaling pathway of bacterial chemotaxis: a molecular view of signal transduction by receptors, kinases, and adaptation enzymes. *Annu. Rev. Cell Dev. Biol.* 13:457–512
- Fauci LJ, Dillon R. 2006. Biofluidmechanics of reproduction. *Annu. Rev. Fluid Mech.* 38:371–94

- Flores H, Lobaton E, Mendez-Diez S, Tlupova S, Cortez R. 2005. A study of bacterial flagellar bundling. *Bull. Math. Biol.* 67:137–68
- Frymier PD, Ford RM, Berg HC, Cummings PT. 1995. Three-dimensional tracking of motile bacteria near a solid planar surface. *PNAS* 92:6195–99
- Fu HC, Powers TR, Wolgemuth HC. 2007. Theory of swimming filaments in viscoelastic media. *Phys. Rev. Lett.* 99:258101
- Fujii M, Shibata S, Aizawa SI. 2008. Polar, peritrichous, and lateral flagella belong to three distinguishable flagellar families. *J. Mol. Biol.* 379:273–83
- Gachelin J, Miño G, Berther H, Lindner A, Rousselet A, Clément E. 2013. Non-Newtonian viscosity of *Escherichia coli* suspensions. *Phys. Rev. Lett.* 110:268103
- Gaffney EA, Gadelha H, Smith DJ, Blake JR, Kirkman-Brown JC. 2011. Mammalian sperm motility: observation and theory. *Annu. Rev. Fluid Mech.* 43:501–28
- Galajda P, Keymer JE, Chaikin P, Austin RH. 2007. A wall of funnels concentrates swimming bacteria. *J. Bacteriol.* 189:8704–7
- Ghosh A, Fischer P. 2009. Controlled propulsion of artificial magnetic nanostructured propellers. *Nano Lett.* 9:2243–45
- Giacché D, Ishikawa T, Yamaguchi T. 2010. Hydrodynamic entrapment of bacteria swimming near a solid surface. *Phys. Rev. E* 82:056309
- Goldstein RE. 2015. Green algae as model organisms for biological fluid dynamics. *Annu. Rev. Fluid Mech.* 47:343–75
- Goldstein SF, Buttle KF, Charon NW. 1996. Structural analysis of the *Leptospiraceae* and *Borrelia burgdorferi* by high-voltage electron microscopy. *J. Bacteriol.* 178:6539–45
- Gray J, Hancock GJ. 1955. The propulsion of sea-urchin spermatozoa. *J. Exp. Biol.* 32:802–14
- Greenberg EP, Canale-Parola E. 1977. Motility of flagellated bacteria in viscous environments. *J. Bacteriol.* 132:356–58
- Guasto JS, Rusconi R, Stocker R. 2012. Fluid mechanics of planktonic microorganisms. *Annu. Rev. Fluid Mech.* 44:373–400
- Haines BM, Sokolov A, Aranson IS, Berlyand L, Karpeev DA. 2009. Three-dimensional model for the effective viscosity of bacterial suspensions. *Phys. Rev. E* 80:041922
- Hancock GJ. 1953. The self-propulsion of microscopic organisms through liquids. *Proc. R. Soc. A* 217:96–121
- Harshey RM. 2003. Bacterial motility on a surface: many ways to a common goal. *Annu. Rev. Microbiol.* 57:249–73
- Hasegawa K, Yamashita I, Namba K. 1998. Quasi- and nonequivalence in the structure of bacterial flagellar filament. *Biophys. J.* 74:569–75
- Hernandez-Ortiz JP, Stoltz CG, Graham MD. 2005. Transport and collective dynamics in suspensions of confined swimming particles. *Phys. Rev. Lett.* 95:204501
- Higdon JJL. 1979. Hydrodynamics of flagellar propulsion: helical waves. *J. Fluid Mech.* 94:331–51
- Hill J, Kalkanci O, McMurry JL, Koser H. 2007. Hydrodynamic surface interactions enable *Escherichia coli* to seek efficient routes to swim upstream. *Phys. Rev. Lett.* 98:068101
- Hotani H. 1980. Micro-video study of moving bacterial flagellar filaments. II. Polymorphic transition in alcohol. *Biosystems* 12:325–30
- Hotani H. 1982. Micro-video study of moving bacterial flagellar filaments. III. Cyclic transformation induced by mechanical force. *J. Mol. Biol.* 156:791–806
- Hyon Y, Marcos, Powers TR, Stocker R, Fu HC. 2012. The wiggling trajectories of bacteria. *J. Fluid Mech.* 705:58–76
- Imhoff JF, Trüper HG. 1977. *Ectothiorhodospira halochloris* sp. nov., a new extremely halophilic phototrophic bacterium containing bacteriochlorophyll b. *Arch. Microbiol.* 114:115–21
- Ishikawa T, Sekiya G, Imai Y, Yamaguchi T. 2007. Hydrodynamic interaction between two swimming bacteria. *Biophys. J.* 93:2217–25
- Janssen PJA, Graham MD. 2011. Coexistence of tight and loose bundled states in a model of bacterial flagellar dynamics. *Phys. Rev. E* 84:011910

- Jarrell KF, McBride MJ. 2008. The surprisingly diverse ways that prokaryotes move. *Nat. Rev. Microbiol.* 6:466–76
- Johnson RE. 1980. An improved slender body theory for Stokes flow. *J. Fluid Mech.* 99:411–31
- Johnson RE, Brokaw CJ. 1979. Flagellar hydrodynamics: a comparison between resistive-force theory and slender-body theory. *Biophys. J.* 25:113–27
- Kaiser GE, Doetsch RN. 1975. Enhanced translational motion of *Leptospira* in viscous environments. *Nature* 255:656–57
- Kanehl P, Ishikawa T. 2014. Fluid mechanics of swimming bacteria with multiple flagella. *Phys. Rev. E* 89:042704
- Kasyap TV, Koch DL, Wu M. 2014. Hydrodynamic tracer diffusion in suspensions of swimming bacteria. *Phys. Fluids* 26:081901
- Kaya T, Koser H. 2009. Characterization of hydrodynamic surface interactions of *Escherichia coli* cell bodies in shear flow. *Phys. Rev. Lett.* 103:138103
- Kaya T, Koser H. 2012. Direct upstream motility in *Escherichia coli*. *Biophys. J.* 102:1514–23
- Kearns DB. 2010. A field guide to bacterial swarming motility. *Nat. Rev. Microbiol.* 8:634–44
- Keller JB. 1974. Effect of viscosity on swimming velocity of bacteria. *PNAS* 71:3253–54
- Keller JB, Rubinow SI. 1976. Swimming of flagellated microorganisms. *Biophys. J.* 16:151–70
- Kim MJ, Bird JC, Parys AJV, Breuer KS, Powers TR. 2003. A macroscopic scale model of bacterial flagellar bundling. *PNAS* 100:15481–85
- Kim MJ, Breuer KS. 2004. Enhanced diffusion due to motile bacteria. *Phys. Fluids* 16:L78–81
- Kim MJ, Powers TR. 2004. Hydrodynamic interactions between rotating helices. *Phys. Rev. E* 69:061910
- Kim MJ, Powers TR. 2005. Deformation of a helical filament by flow and electric or magnetic fields. *Phys. Rev. E* 71:021914
- Kim S, Karrila JS. 1991. *Microhydrodynamics: Principles and Selected Applications*. Boston: Butterworth-Heinemann
- Koch DL, Subramanian G. 2011. Collective hydrodynamics of swimming microorganisms: living fluids. *Annu. Rev. Fluid Mech.* 43:637–59
- Lauga E. 2007. Propulsion in a viscoelastic fluid. *Phys. Fluids* 19:083104
- Lauga E. 2014. Locomotion in complex fluids: integral theorems. *Phys. Fluids* 26:081902
- Lauga E, DiLuzio WR, Whitesides GM, Stone HA. 2006. Swimming in circles: motion of bacteria near solid boundaries. *Biophys. J.* 90:400–12
- Lauga E, Powers TR. 2009. The hydrodynamics of swimming microorganisms. *Rep. Prog. Phys.* 72:096601
- Leifson E. 1960. *Atlas of Bacterial Flagellation*. New York: Academic
- Lemelle L, Palierne JF, Chatre E, Vaillant C, Place C. 2013. Curvature reversal of the circular motion of swimming bacteria probes for slip at solid/liquid interfaces. *Soft Matter* 9:9759–62
- Leshansky AM. 2009. Enhanced low-Reynolds-number propulsion in heterogeneous viscous environments. *Phys. Rev. E* 80:051911
- Li G, Tam LK, Tang JX. 2008. Amplified effect of Brownian motion in bacterial near-surface swimming. *PNAS* 105:18355–59
- Liao Q, Subramanian G, DeLisa MP, Koch DL, Wu MM. 2007. Pair velocity correlations among swimming *Escherichia coli* bacteria are determined by force-quadrupole hydrodynamic interactions. *Phys. Fluids* 19:061701
- Lighthill J. 1975. *Mathematical Biofluidynamics*. Philadelphia: SIAM
- Lighthill J. 1976. Flagellar hydrodynamics: the John von Neumann lecture, 1975. *SIAM Rev.* 18:161–230
- Lim S, Peskin CS. 2012. Fluid-mechanical interaction of flexible bacterial flagella by the immersed boundary method. *Phys. Rev. E* 85:036307
- Lin Z, Thiffeault JL, Childress S. 2011. Stirring by squirmers. *J. Fluid Mech.* 669:167–77
- Liu B, Breuer KS, Powers TR. 2013. Helical swimming in Stokes flow using a novel boundary-element method. *Phys. Fluids* 25:061902
- Liu B, Breuer KS, Powers TR. 2014a. Propulsion by a helical flagellum in a capillary tube. *Phys. Fluids* 26:011701
- Liu B, Gulino M, Morse M, Tang JX, Powers TR, Breuer KS. 2014b. Helical motion of the cell body enhances *Caulobacter crescentus* motility. *PNAS* 111:11252–56

- Liu B, Powers TR, Breuer KS. 2011. Force-free swimming of a model helical flagellum in viscoelastic fluids. *PNAS* 108:19516–20
- Lopez D, Lauga E. 2014. Dynamics of swimming bacteria at complex interfaces. *Phys. Fluids* 26:071902
- Lytle DA, Johnson CH, Rice EW. 2002. A systematic comparison of the electrokinetic properties of environmentally important microorganisms in water. *Colloids Surf. B* 24:91–101
- Macnab RM. 1977. Bacterial flagella rotating in bundles: a study in helical geometry. *PNAS* 74:221–25
- Madigan MT, Martinko JM, Stahl D, Clark DP. 2010. *Brock Biology of Microorganisms*. San Francisco: Benjamin Cummings. 13th ed.
- Magariyama Y, Ichiba M, Nakata K, Baba K, Ohtani T, et al. 2005. Difference in bacterial motion between forward and backward swimming caused by the wall effect. *Biophys. J.* 88:3648–58
- Magariyama Y, Kudo S. 2002. A mathematical explanation of an increase in bacterial swimming speed with viscosity in linear-polymer solutions. *Biophys. J.* 83:733–39
- Magariyama Y, Sugiyama S, Kudo S. 2001. Bacterial swimming speed and rotation rate of bundled flagella. *FEMS Microbiol. Lett.* 199:125–29
- Magariyama Y, Sugiyama S, Muramoto K, Kawagishi I, Imae Y, Kudo S. 1995. Simultaneous measurement of bacterial flagellar rotation rate and swimming speed. *Biophys. J.* 69:2154–62
- Männik J, Driessens R, Galajda P, Keymer JE, Dekker C. 2009. Bacterial growth and motility in sub-micron constrictions. *PNAS* 106:14861–66
- Marcos, Fu HC, Powers TR, Stocker R. 2012. Bacterial rheotaxis. *PNAS* 109:4780–85
- Martinez VA, Schwarz-Linek J, Reufer M, Wilson LG, Morozov AN, Poon WCK. 2014. Flagellated bacterial motility in polymer solutions. *PNAS* 111:17771–76
- Miño GL, Dunstan J, Rousselet A, Clément E, Soto R. 2013. Induced diffusion of tracers in a bacterial suspension: theory and experiments. *J. Fluid Mech.* 729:423–44
- Mitchell JG. 2002. The energetics and scaling of search strategies in bacteria. *Am. Nat.* 160:727–40
- Morse M, Huang A, Li G, Maxey MR, Tang JX. 2013. Molecular adsorption steers bacterial swimming at the air/water interface. *Biophys. J.* 105:21–28
- Namba K, Vonderviszt F. 1997. Molecular architecture of bacterial flagellum. *Q. Rev. Biophys.* 30:1–65
- Olson SD, Lim S, Cortez R. 2013. Modeling the dynamics of an elastic rod with intrinsic curvature and twist using a regularized Stokes formulation. *J. Comp. Phys.* 238:169–87
- Ottemann KM, Miller JF. 1997. Roles for motility in bacterial-host interactions. *Mol. Microbiol.* 24:1109–17
- Pedley TJ, Kessler JO. 1992. Hydrodynamic phenomena in suspensions of swimming microorganisms. *Annu. Rev. Fluid Mech.* 24:313–58
- Phan-Thien N, Tran-Cong T, Ramia M. 1987. A boundary-element analysis of flagellar propulsion. *J. Fluid Mech.* 184:533–49
- Purcell EM. 1977. Life at low Reynolds number. *Am. J. Phys.* 45:3–11
- Purcell EM. 1997. The efficiency of propulsion by a rotating flagellum. *PNAS* 94:11307–11
- Pushkin DO, Shum H, Yeomans JM. 2013. Fluid transport by individual microswimmers. *J. Fluid Mech.* 726:5–25
- Qian B, Jiang H, Gagnon DA, Breuer KS, Powers TR. 2009. Minimal model for synchronization induced by hydrodynamic interactions. *Phys. Rev. E* 80:061919
- Ramia M, Tullock DL, Phan-Thien N. 1993. The role of hydrodynamic interaction in the locomotion of microorganisms. *Biophys. J.* 65:755–78
- Reichert M, Stark H. 2005. Synchronization of rotating helices by hydrodynamic interactions. *Eur. Phys. J. E* 17:493–500
- Reid SW, Leake MC, Chandler JH, Lo CJ, Armitage JP, Berry RM. 2006. The maximum number of torque-generating units in the flagellar motor of *Escherichia coli* is at least 11. *PNAS* 103:8066–71
- Reigh SY, Winkler RG, Gompper G. 2012. Synchronization and bundling of anchored bacterial flagella. *Soft Matter* 8:4363–72
- Rusconi R, Guasto JS, Stocker R. 2014. Bacterial transport suppressed by fluid shear. *Nat. Phys.* 10:212–17
- Saintillan D. 2010a. Extensional rheology of active suspensions. *Phys. Rev. E* 81:056307
- Saintillan D. 2010b. The dilute rheology of swimming suspensions: a simple kinetic model. *J. Exp. Mech.* 50:1275–81

- Schneider W, Doetsch RN. 1974. Effect of viscosity on bacterial motility. *J. Bacteriol.* 117:696–701
- Schnitzer MJ. 1993. Theory of continuum random walks and application to chemotaxis. *Phys. Rev. E* 48:2553–68
- Shaevitz JW, Lee JY, Fletcher DA. 2005. *Spiroplasma* swim by a processive change in body helicity. *Cell* 122:941–45
- Shoemaker JG. 1960. The measurement of bacterial motility. *J. Gen. Microbiol.* 22:528–35
- Silverman M, Simon M. 1974. Flagellar rotation and the mechanism of bacterial motility. *Nature* 249:73–74
- Sokolov A, Apodaca MM, Grzybowski BA, Aranson IS. 2010. Swimming bacteria power microscopic gears. *PNAS* 107:969–74
- Sokolov A, Aranson IS. 2009. Reduction of viscosity in suspension of swimming bacteria. *Phys. Rev. Lett.* 103:148101
- Son K, Guasto JS, Stocker R. 2013. Bacteria can exploit a flagellar buckling instability to change direction. *Nat. Phys.* 9:494–98
- Spagnolie SE, ed. 2015. *Complex Fluids in Biological Systems*. New York: Springer
- Spagnolie SE, Lauga E. 2011. Comparative hydrodynamics of bacterial polymorphism. *Phys. Rev. Lett.* 106:058103
- Spagnolie SE, Lauga E. 2012. Hydrodynamics of self-propulsion near a boundary: predictions and accuracy of far-field approximations. *J. Fluid Mech.* 700:105–47
- Spagnolie SE, Liu B, Powers TR. 2013. Locomotion of helical bodies in viscoelastic fluids: enhanced swimming at large helical amplitudes. *Phys. Rev. Lett.* 111:068101
- Sririraj SV, Powers TR. 2006. Model for polymorphic transitions in bacterial flagella. *Phys. Rev. E* 73:011902
- Stocker R, Seymour JR. 2012. Ecology and physics of bacterial chemotaxis in the ocean. *Microbiol. Mol. Biol. Rev.* 76:792–812
- Taylor GI. 1967. Low-Reynolds-number flows. US Natl. Comm. Fluid Mech. Films video. <https://www.youtube.com/watch?v=51-6QCJTAjU>
- Thomas D, Morgan DG, DeRosier DJ. 2001. Structures of bacterial flagellar motors from two FliF-FliG gene fusion mutants. *J. Bacteriol.* 183:6404–12
- Turner L, Ryu WS, Berg HC. 2000. Real-time imaging of fluorescent flagellar filaments. *J. Bacteriol.* 182:2793–801
- Vanloosdrecht MCM, Lyklema J, Norde W, Zehnder AJB. 1990. Influence of interfaces on microbial activity. *Microbiol. Rev.* 54:75–87
- Vig DK, Wolgemuth CW. 2012. Swimming dynamics of the Lyme disease spirochete. *Phys. Rev. Lett.* 109:218104
- Vigeant MAS, Ford RM. 1997. Interactions between motile *Escherichia coli* and glass in media with various ionic strengths, as observed with a three-dimensional tracking microscope. *Appl. Environ. Microbiol.* 63:3474–79
- Vogel R, Stark H. 2010. Force-extension curves of bacterial flagella. *Eur. Phys. J. E* 33:259–71
- Vogel R, Stark H. 2012. Motor-driven bacterial flagella and buckling instabilities. *Eur. Phys. J. E* 35:15
- Vogel R, Stark H. 2013. Rotation-induced polymorphic transitions in bacterial flagella. *Phys. Rev. Lett.* 110:158104
- Vogel S. 1996. *Life in Moving Fluids*. Princeton, NJ: Princeton Univ. Press
- Wada H, Netz RR. 2007. Model for self-propulsive helical filaments: kink-pair propagation. *Phys. Rev. Lett.* 99:108102
- Wada H, Netz RR. 2008. Discrete elastic model for stretching-induced flagellar polymorphs. *Eur. Phys. Lett.* 82:28001
- Watari N, Larson RG. 2010. The hydrodynamics of a run-and-tumble bacterium propelled by polymorphic helical flagella. *Biophys. J.* 98:12–17
- Weibull C. 1950. Electrophoretic and titrimetric measurements on bacterial flagella. *Acta Chem. Scand.* 4:260–67
- Wilking JN, Angelini TE, Seminara A, Brenner MP, Weitz DA. 2011. Biofilms as complex fluids. *MRS Bull.* 36:385–91
- Wolfe AJ, Conley MP, Berg HC. 1988. Acetyladenylate plays a role in controlling the direction of flagellar rotation. *PNAS* 85:6711–15

- Wu XL, Libchaber A. 2000. Particle diffusion in a quasi-two-dimensional bacterial bath. *Phys. Rev. Lett.* 84:3017–20
- Xie L, Altindal T, Chattopadhyay S, Wu XL. 2011. Bacterial flagellum as a propeller and as a rudder for efficient chemotaxis. *PNAS* 108:2246–51
- Yuan J, Fahrner KA, Turner L, Berg HC. 2010. Asymmetry in the clockwise and counterclockwise rotation of the bacterial flagellar motor. *PNAS* 107:12846–49
- Zhang L, Peyer KE, Nelson BJ. 2010. Artificial bacterial flagella for micromanipulation. *Lab Chip* 10:2203–15
- Zhou S, Sokolov S, Lavrentovich OD, Aranson IS. 2014. Living liquid crystals. *PNAS* 111:1265–70

## Contents

Biomimetic Survival Hydrodynamics and Flow Sensing <i>Michael S. Triantafyllou, Gabriel D. Weymouth, and Jianmin Miao</i>	1
Motion and Deformation of Elastic Capsules and Vesicles in Flow <i>Dominique Barthès-Biesel</i>	25
High-Reynolds Number Taylor-Couette Turbulence <i>Siegfried Grossmann, Detlef Lohse, and Chao Sun</i>	53
Shear Banding of Complex Fluids <i>Thibaut Divoux, Marc A. Fardin, Sébastien Manneville, and Sandra Lerouge</i>	81
Bacterial Hydrodynamics <i>Eric Lauga</i>	105
Quadrant Analysis in Turbulence Research: History and Evolution <i>James M. Wallace</i>	131
Modeling of Fine-Particle Formation in Turbulent Flames <i>Venkat Raman and Rodney O. Fox</i>	159
Seismic Sounding of Convection in the Sun <i>Shravan Hanasoge, Laurent Gizon, and Katepalli R. Sreenivasan</i>	191
Cerebrospinal Fluid Mechanics and Its Coupling to Cerebrovascular Dynamics <i>Andreas A. Linninger, Kevin Tangen, Chih-Yang Hsu, and David Frim</i>	219
Fluid Mechanics of Heart Valves and Their Replacements <i>Fotis Sotiropoulos, Trung Bao Le, and Anvar Gilmanov</i>	259
Droplets and Bubbles in Microfluidic Devices <i>Shelley Lynn Anna</i>	285
Mechanics of Hydraulic Fractures <i>Emmanuel Detournay</i>	311
A Normal Mode Perspective of Intrinsic Ocean-Climate Variability <i>Henk Dijkstra</i>	341
Drop Impact on a Solid Surface <i>C. Josserand and S.T. Thoroddsen</i>	365

Contrail Modeling and Simulation <i>Roberto Paoli and Karim Shariff</i> .....	393
Modeling Nonequilibrium Gas Flow Based on Moment Equations <i>Manuel Torrilhon</i> .....	429
The Fluid Mechanics of Pyroclastic Density Currents <i>Josef Dufek</i> .....	459
The Dynamics of Microtubule/Motor-Protein Assemblies in Biology and Physics <i>Michael J. Shelley</i> .....	487
Dynamics and Instabilities of Vortex Pairs <i>Thomas Leweke, Stéphane Le Dizès, and Charles H.K. Williamson</i> .....	507

## Indexes

Cumulative Index of Contributing Authors, Volumes 1–48 .....	543
Cumulative Index of Article Titles, Volumes 1–48 .....	553

## Errata

An online log of corrections to *Annual Review of Fluid Mechanics* articles may be found at <http://www.annualreviews.org/errata/fluid>